

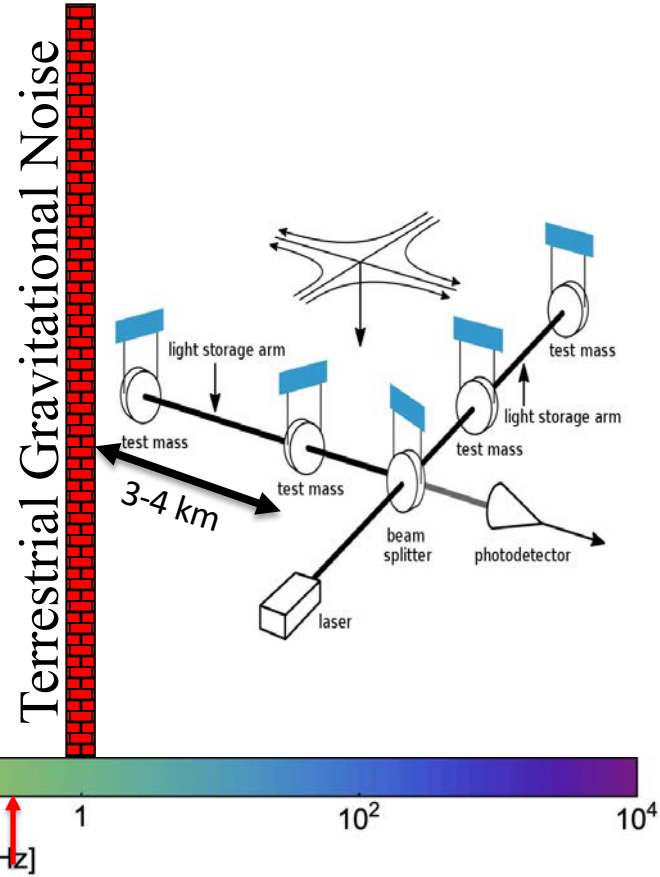
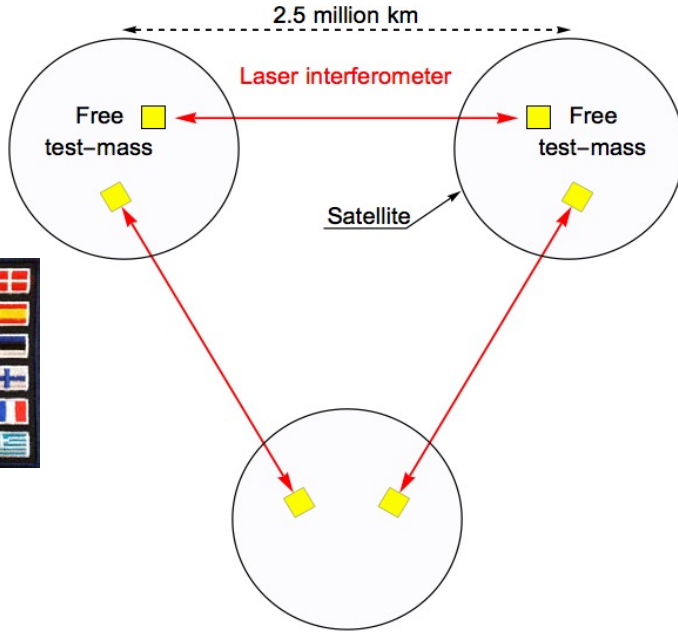
# The LISA mission

[Stefano.Vitale@unitn.it](mailto:Stefano.Vitale@unitn.it)

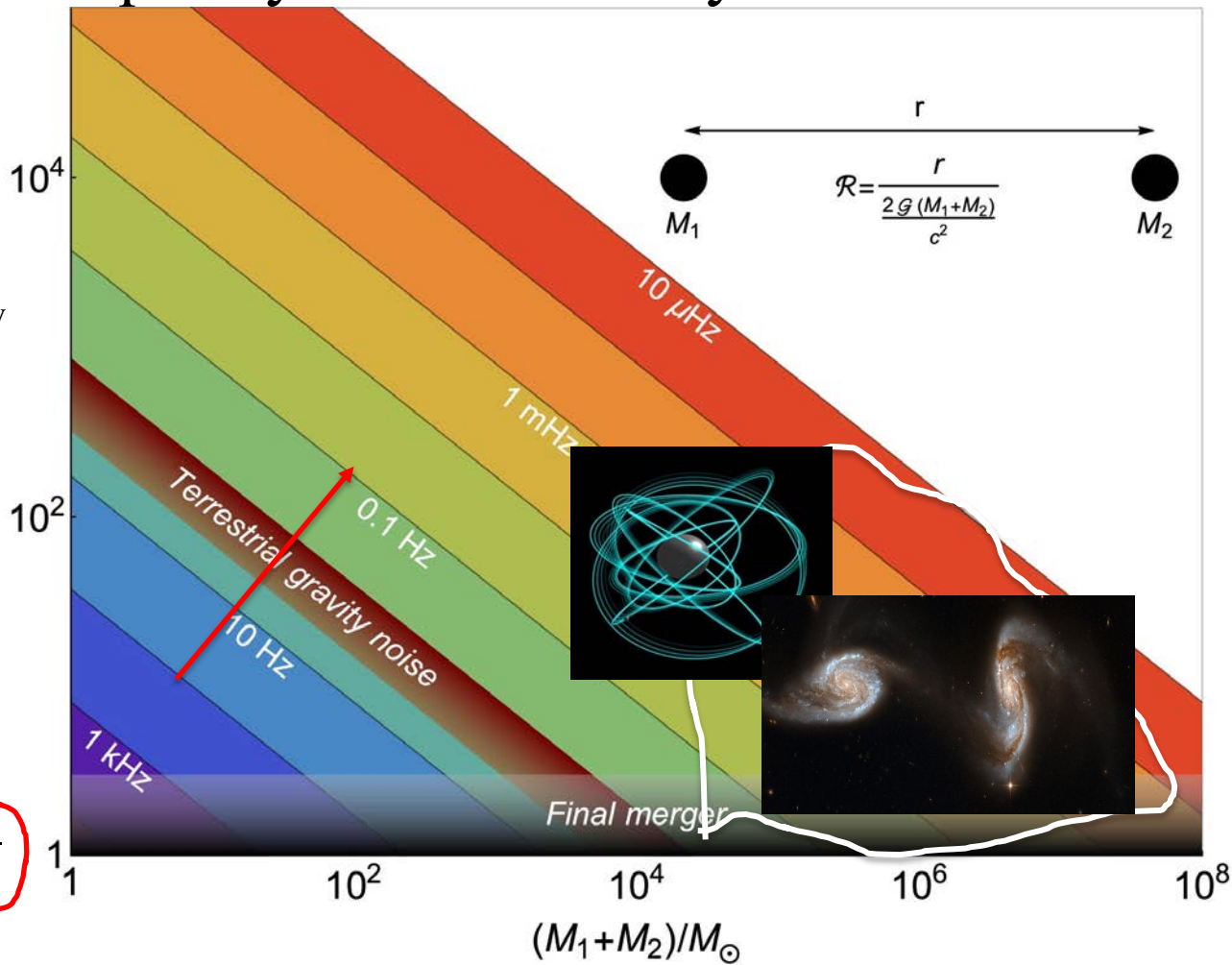
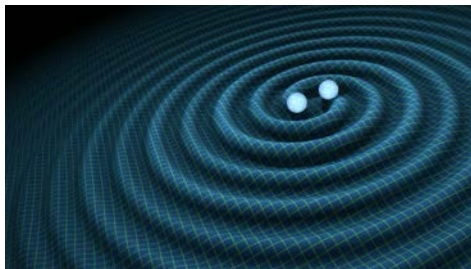
Università di Trento, Istituto Nazionale di Fisica

S. Vitale Nucleare and Agenzia Spaziale Italiana

# LISA: the quest for low-frequency GW



# Low frequency GW astronomy



- Binaries are nearly Keplerian, frequency of wave twice frequency of revolution

$$f_{GW} = \frac{1}{\pi} \sqrt{\frac{G(M_1 + M_2)}{r^3}} \quad \mathcal{R}$$

- Separation normalized to Schwarzschild radii:

$$\mathcal{R} = \frac{r}{\left(\frac{2G(M_1 + M_2)}{c^2}\right)}$$

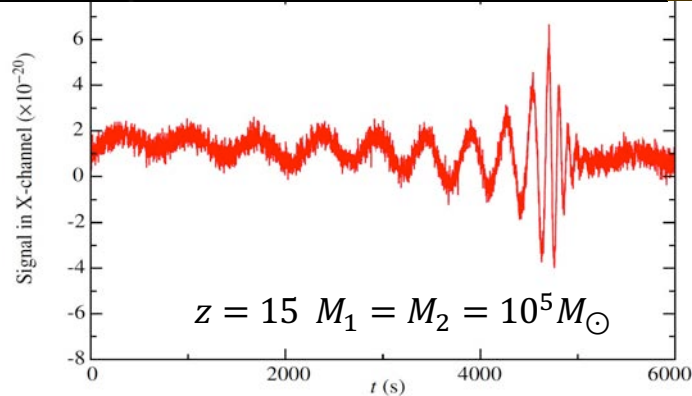
( $\mathcal{R} \rightarrow 1 \simeq$  final merger)

- Frequency decreases with both mass and  $\mathcal{R}$

$$f_{GW} = \frac{c}{\pi\sqrt{2} R_{\odot}} \left(\frac{M_1 + M_2}{M_{\odot}}\right)^{-1} \mathcal{R}^{-\frac{3}{2}}$$

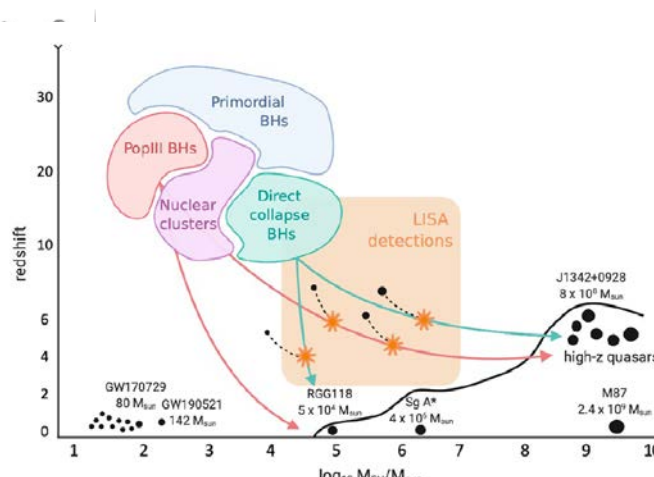
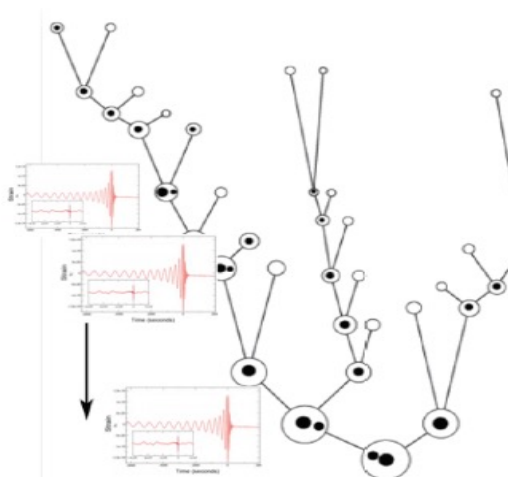
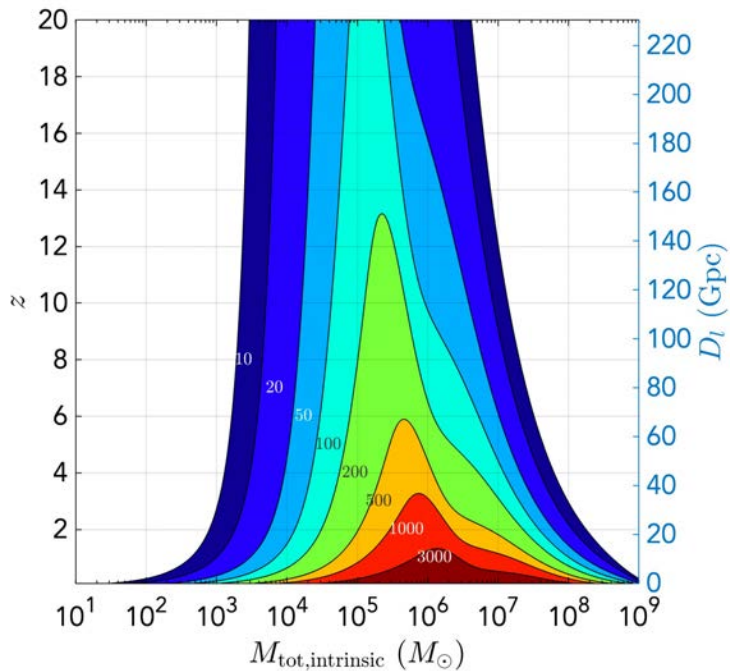
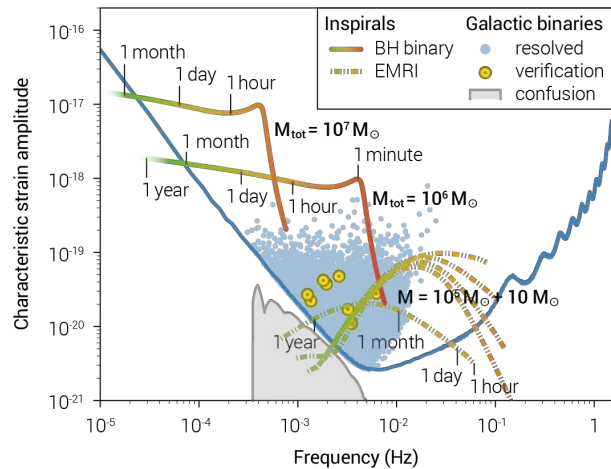
# Supermassive BH mergers: the brightest sources

- Wave amplitude scales with  $M_1 \times M_2$ : detectable “everywhere” in the universe



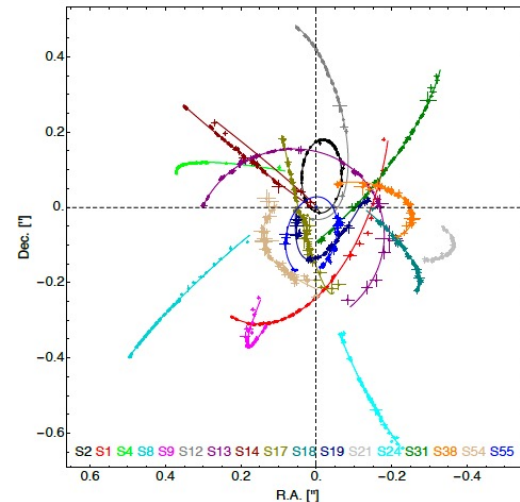
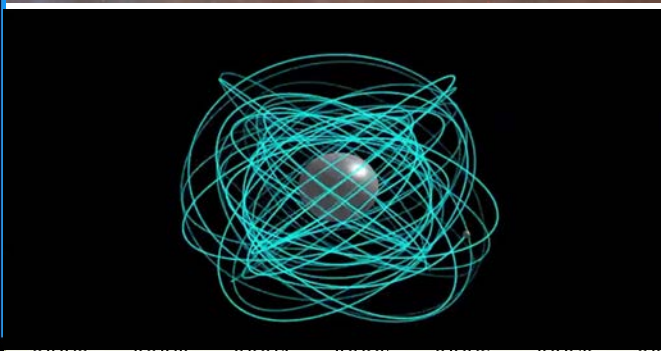
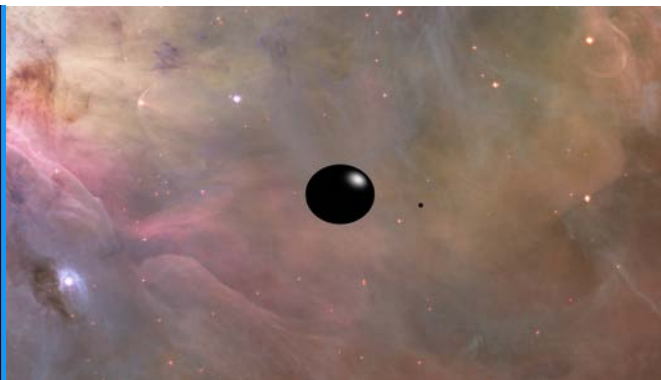
# Supermassive BH mergers: the brightest sources

- Detectable “everywhere” in the universe
- Sooner or later frequency crosses LISA band : cosmological stratigraphy

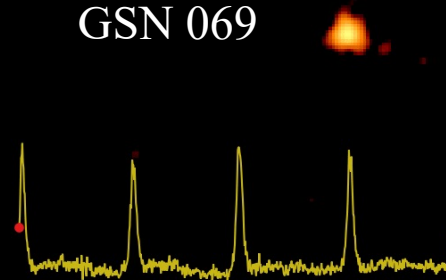


# Extreme Mass Ratio Inspirals

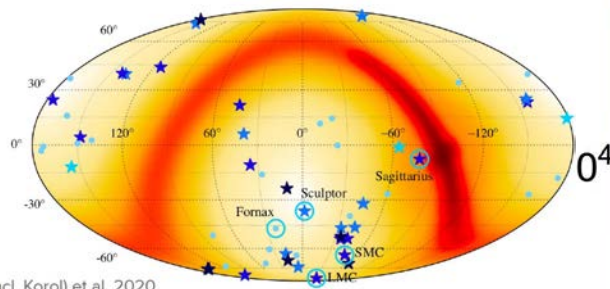
- Inspiral of stellar-mass compact object (CO) into massive black hole (MBH): Hills & Bender 95
  - ✦ MBH mass  $10^4 < M/M_\odot < 10^7$
  - ✦ Up to  $10^4$ - $10^5$  cycles in band
  - ✦ If CO is a white dwarf, possible electromagnetic counterpart (Zalamea+10)
- Gravitational waves encode precise information on CO and MBH:
  - ✦  $M_{\text{BH}}(1+z)$ ,  $a_{\text{BH}}$  measurable to extreme precision
  - ✦ Detectable to  $z \sim \text{few}$ ; sky localization  $\sim 1$ - $10 \text{ deg}^2$  (Babak+17)
- Precise mapping of MBH spacetime
  - ✦ MBH multipole measurement  $\rightarrow$  test of no-hair theorem (Ryan 95)



XMM-Newton  
GSN 069

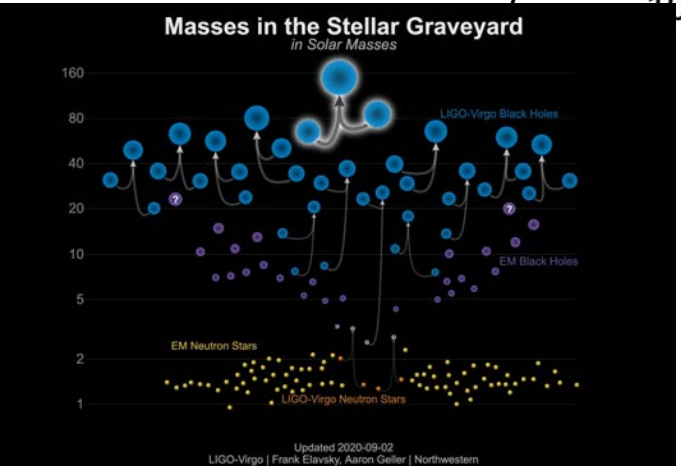
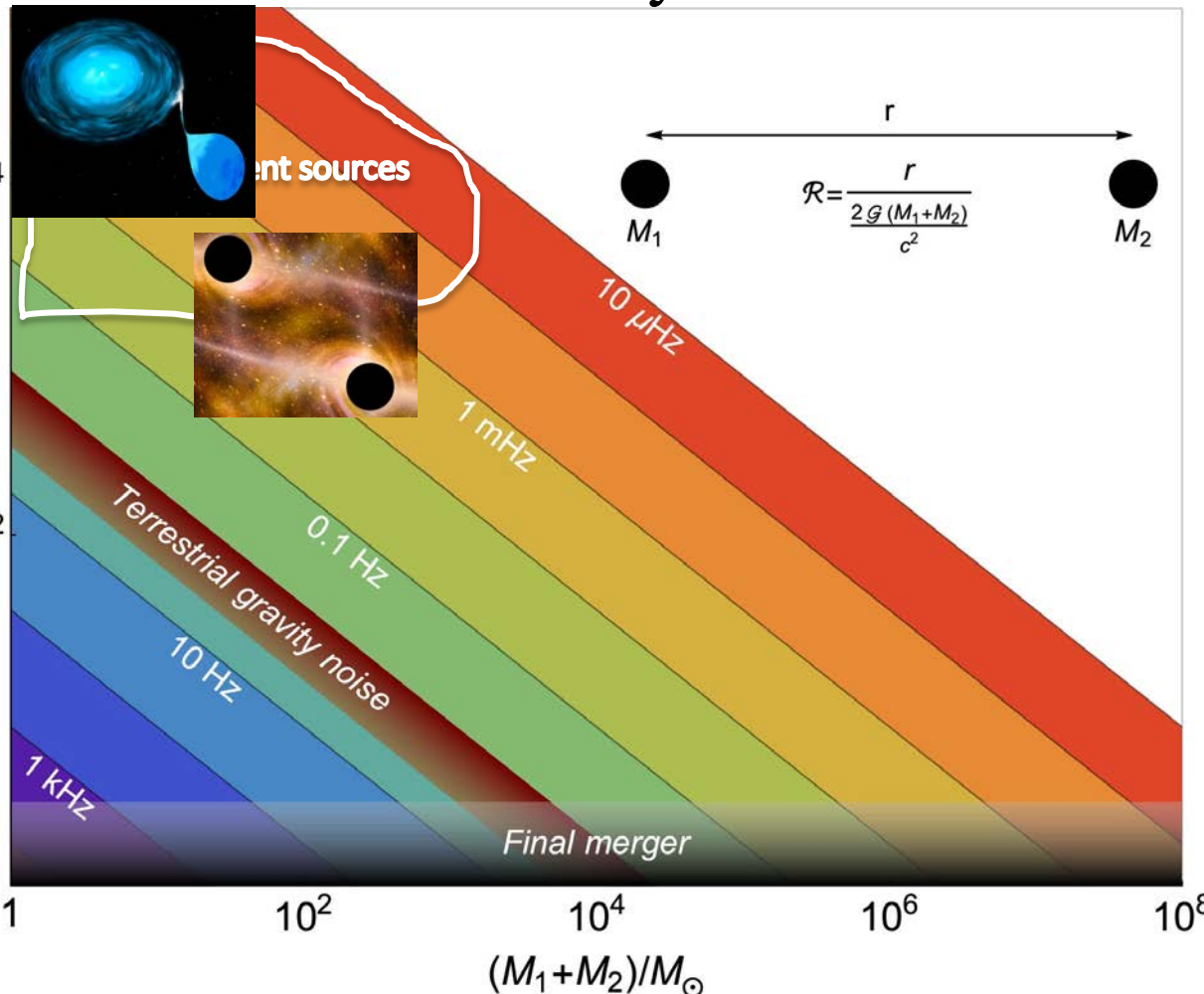


# Non-transient GW astronomy



Roebber (incl. Korol) et al. 2020

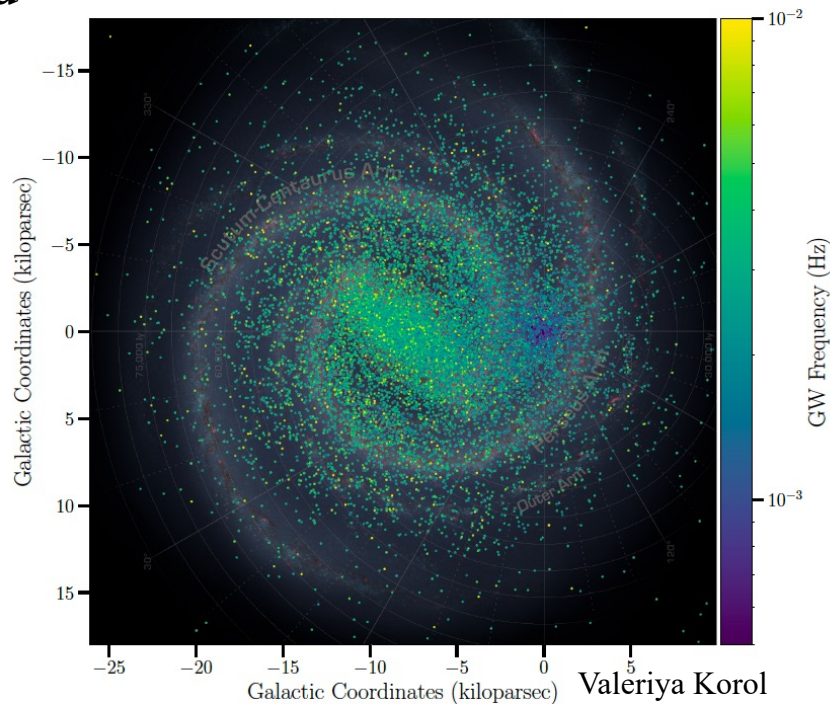
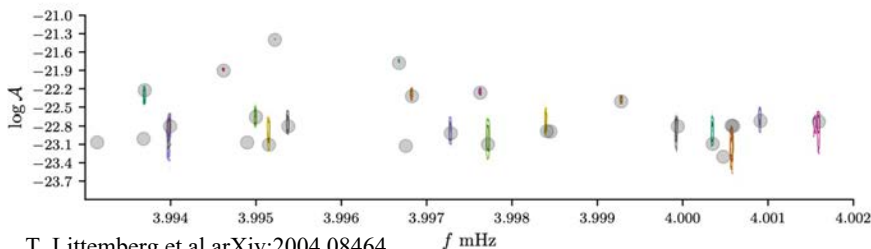
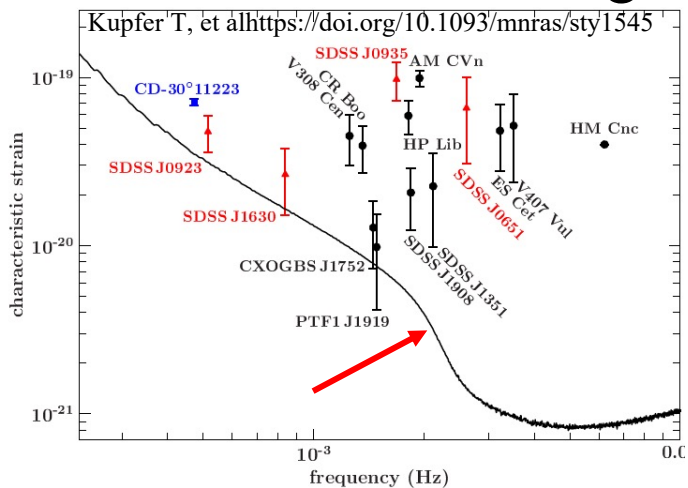
- GW-binary astronomy of local group
- BH multi-band astronomy



Updated 2020-09-02  
LIGO-Virgo | Frank Elavsky, Aaron Geller | Northwestern

# The high $\mathcal{R}$ end: the GW Milky Way

- Tens of thousand of discernible sources
- Plus a stochastic foreground



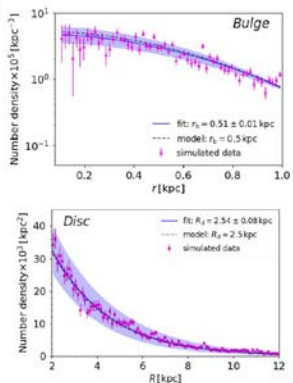


## The shape of the Milky Way's components

The spatial distribution of DWDs with measured distances (several thousand) constrains:

- Bulge scale radius to 2%
- Disc scale radius to 3%
- Disc scale height to 16%

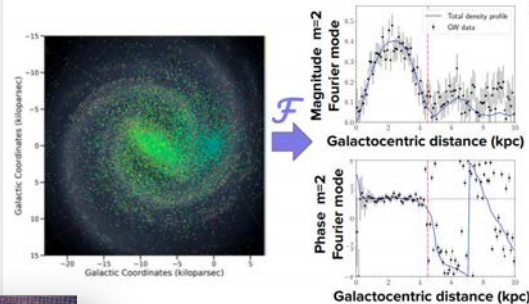
Korol et al 2019  
See also Adams et al. 2012



# Expectations

## Structural parameters of the central bar

Fourier transformation of the DWD spatial distribution can reveal shape of the bar.



Specifically, it will constrain:

- axis ratio to 10%
- length to < 1%
- orientation angle to < 1°

(Wilhelm, Korol et al. 2020)

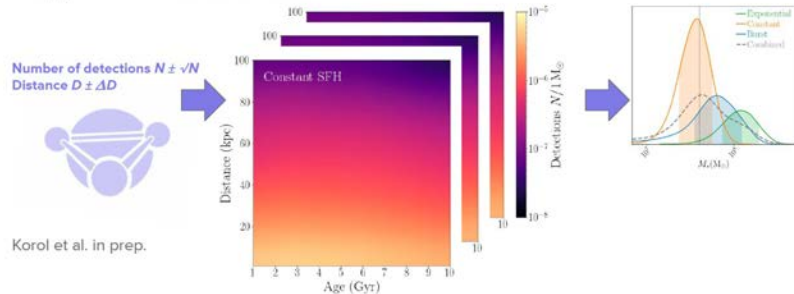


The detection of circumbinary exoplanets

Camilla DANIELSKI

## Weighing Milky Way satellites

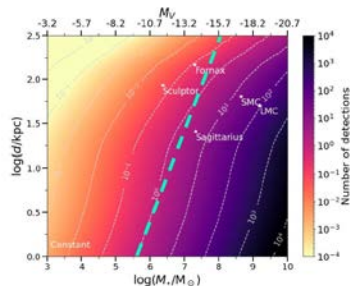
By exploiting our models we can recover the satellite's total stellar mass: to within a factor two if SFH is known and to an order of magnitude when marginalising over different SFH models. If no detections are identified with the satellite we can still place an upper limit on its stellar mass.



Korol et al. in prep.

## Discovering Milky Way satellites in gravitational waves

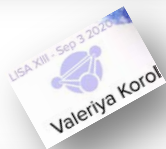
- Satellites with stellar mass  $> 10^6 M_{\odot}$  host detectable LISA sources
- LISA detections can inform us about the total stellar mass and star formation history of the satellites
- Discovery of satellites invisible to electromagnetic observatories



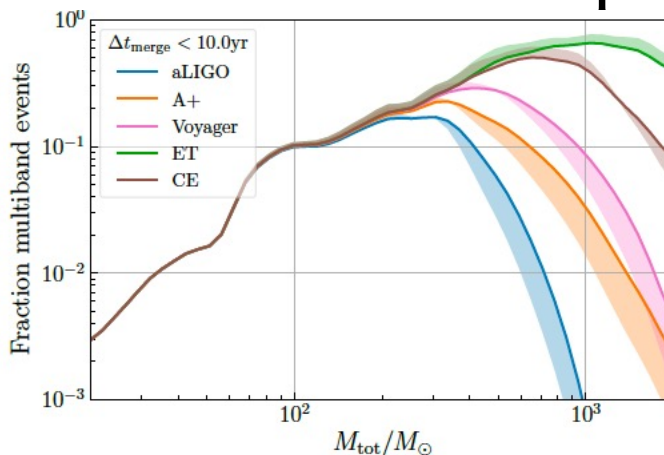
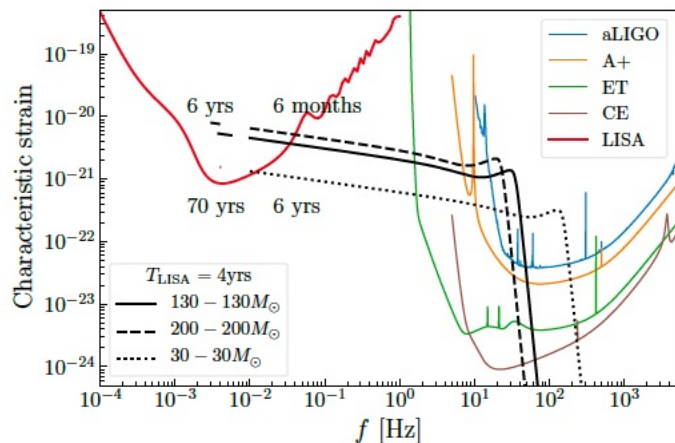
See talk by Riccardo Buscicchio

Korol et al. 2020; Roebber et al. (incl.Korol) 2020  
See also Lamberts et al. 2019

S. Vitale



# Multi-band GW astronomy and fundamental physics



Joint observation greatly improves measurement of deviation from GR

S. Datta et al arXiv:2006.12137v1 [gr-qc] 22 Jun 2020

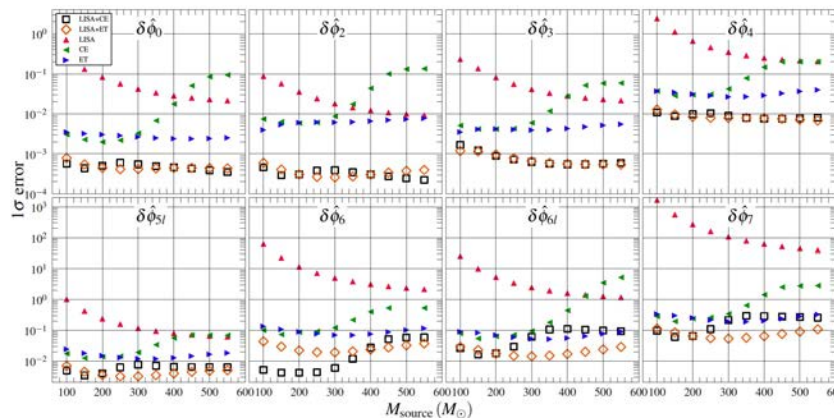


FIG. 3. Top panel shows bounds on deformation parameters at 2.5PN to 2PN, as a function of total mass in source frame. Bottom panel shows the same but for deformation parameters at 2.5PN to 3.5PN. All the systems have mass-ratio  $q = 2$ , dimensionless component spins  $\chi_1 = 0.2$  and  $\chi_2 = 0.1$ , and luminosity distance  $D_L = 1$  Gpc.

# Interesting reading

## Astrophysics with the Laser Interferometer Space Antenna

## Cosmology with the Laser Interferometer Space Antenna

Contents	
General Introduction . . . . .	3
<b>1 Stellar Compact Binaries and Multiples . . . . .</b>	<b>5</b>
1.1 Introduction and Summary . . . . .	6
1.2 Classes of LISA binaries . . . . .	8
1.2.1 Known binaries — LISA verification sources . . . . .	8
1.2.2 Detached binaries . . . . .	13
1.2.2.1 WD+WD systems . . . . .	13
1.2.2.2 NS+WD and BH+WD systems . . . . .	14
1.2.2.3 NS+NS systems . . . . .	15
1.2.2.4 BH+NS and BH+BH systems . . . . .	16
1.2.2.5 Stochastic background . . . . .	17
1.2.3 Interacting binaries . . . . .	17
1.2.3.1 AM CVn binaries (AM Canum Venaticorum binaries — accreting WDs) . . . . .	17
1.2.3.2 UCXBs (ultra-compact X-ray binaries) . . . . .	19
1.2.4 Other potential sources . . . . .	20
1.2.4.1 Helium-star binaries . . . . .	20
1.2.4.2 Period bouncing CVs . . . . .	22
1.2.4.3 Exoplanets, brown dwarfs and substellar companions . . . . .	22

Contents	
<b>1 Introduction . . . . .</b>	<b>8</b>
<b>2 Tests of cosmic expansion and acceleration with standard sirens . . . . .</b>	<b>11</b>
2.1 Introduction . . . . .	11
2.2 Standard sirens . . . . .	11
2.2.1 Bright sirens: MBBHs with electromagnetic counterpart . . . . .	12
2.2.2 Dark sirens: SOBBH, EMRIs, IMBBHs . . . . .	13
2.2.3 Systematic uncertainties on standard sirens . . . . .	15
2.3 Constraints on $\Lambda$ CDM . . . . .	16
2.3.1 $H_0$ tension and standard sirens . . . . .	16
2.3.2 LISA forecast for $H_0$ . . . . .	17
2.3.3 $\Lambda$ CDM beyond $H_0$ . . . . .	18
2.3.4 Tests of $\Lambda$ CDM at high-redshift . . . . .	19
2.4 Probing dark energy . . . . .	20
2.4.1 Equation of state of dark energy: $w_0$ and $w_a$ . . . . .	20
2.4.2 Alternative dark energy models . . . . .	20
2.5 Synergy with other cosmological measurements . . . . .	21
2.5.1 Integration with standard electromagnetic observations . . . . .	21
2.5.2 Complementarity with other gravitational wave observatories . . . . .	21
2.6 Cross-correlation and interaction with large scale structure . . . . .	22
2.6.1 Cross-correlations with resolved events . . . . .	23
2.6.2 Cross-correlations with the stochastic gravitational wave background . . . . .	24
2.6.3 Large-scale structure effects on gravitational-wave luminosity distance estimates . . . . .	26

\*Section coordinator. More details at the beginning of each section.  
†Document coordinator.

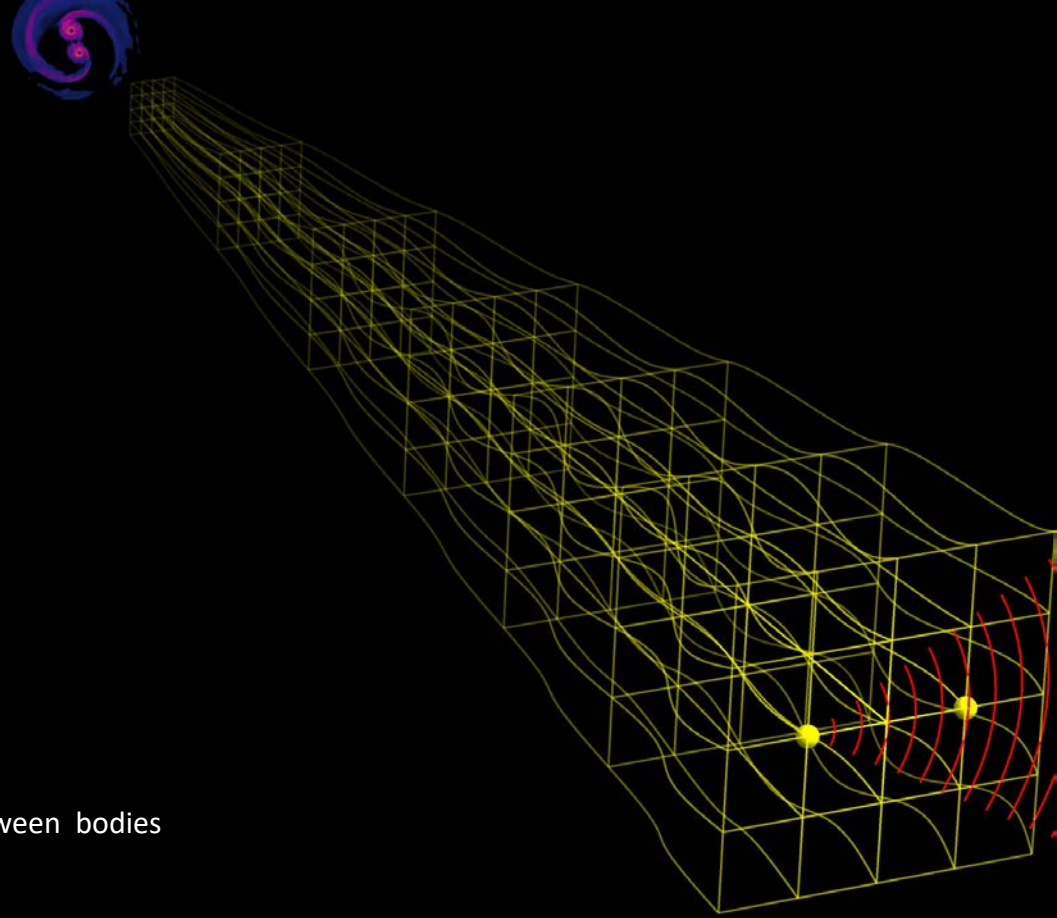
arXiv:2204.05434v1 [astro-ph.CO] 11 Apr 2022

arXiv:2203.06016v1 [gr-qc] 11 Mar 2022

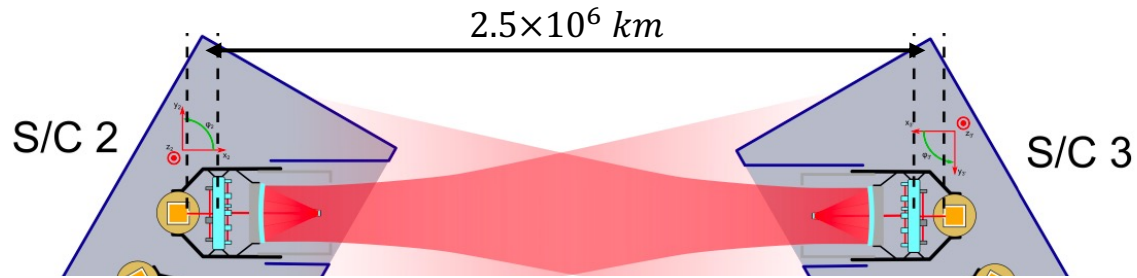
# Detecting gravitational wave in space

- Waves of space-time curvature that propagate at speed of light
- Doppler tracking of free orbiting bodies modulated at period of gravitational wave

$$\frac{\Delta \dot{v}}{v_0} \approx c \underbrace{R^x_{0x0} L}_{\substack{\text{Curvature} \\ \text{tensor}}} \left. \vphantom{R^x_{0x0} L} \right\} \text{Separation between bodies}$$

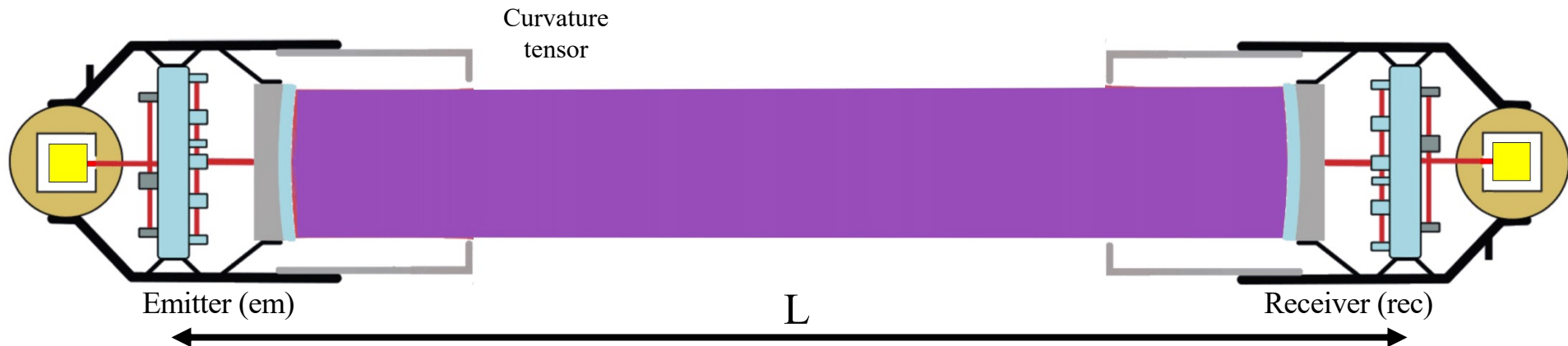


# LISA



# The LISA link

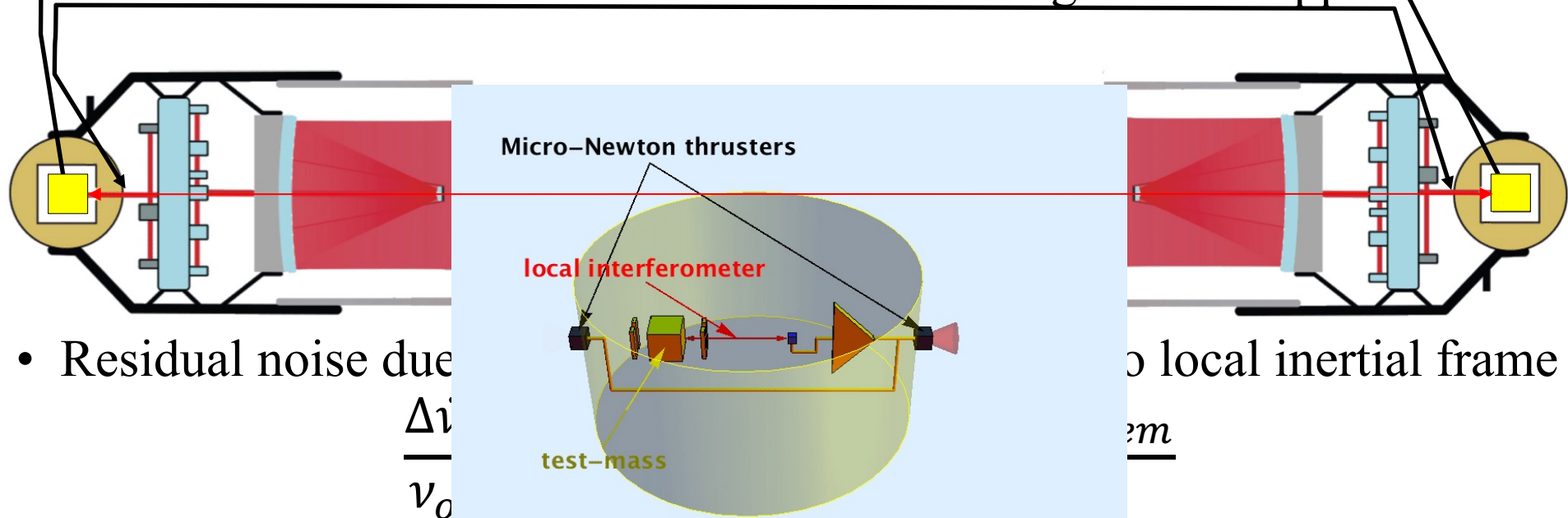
- Propagating throughout GW curvature, beam accumulates a time modulated frequency shift  $\frac{\Delta \dot{\nu}}{\nu_0} \simeq \underbrace{c R^x_{0x0} L}_{\text{Curvature tensor}} \underbrace{\quad}_{\text{Size of detector}}$



- Acceleration of spacecraft via standard Doppler effect also shifts frequency and mimics GW  $\frac{\Delta \dot{\nu}}{\nu_0} = c R^x_{0x0} L + \frac{a_{rec} - a_{em}}{c}$
- Spacecraft (S/C) accelerate too much because of solar radiation pressure

# Coping with S/C acceleration

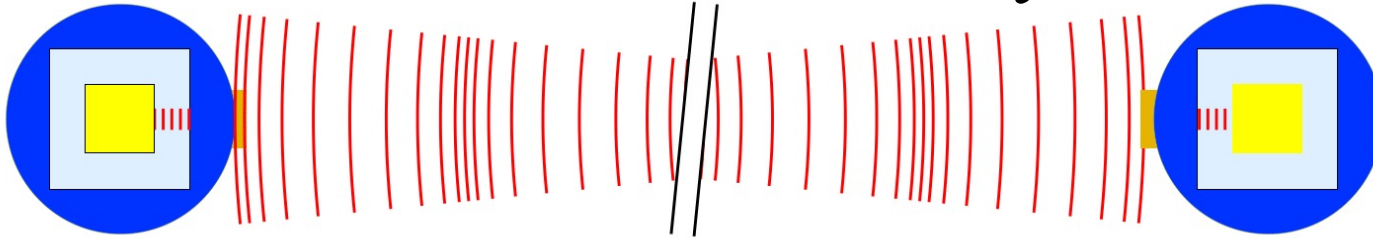
- Free-floating test-masses (TM) are carried inside S/C
- No contact between TM and S/C, “drag-free” along the beam
- Measure S/C-to-TM acceleration and correct signal for Doppler



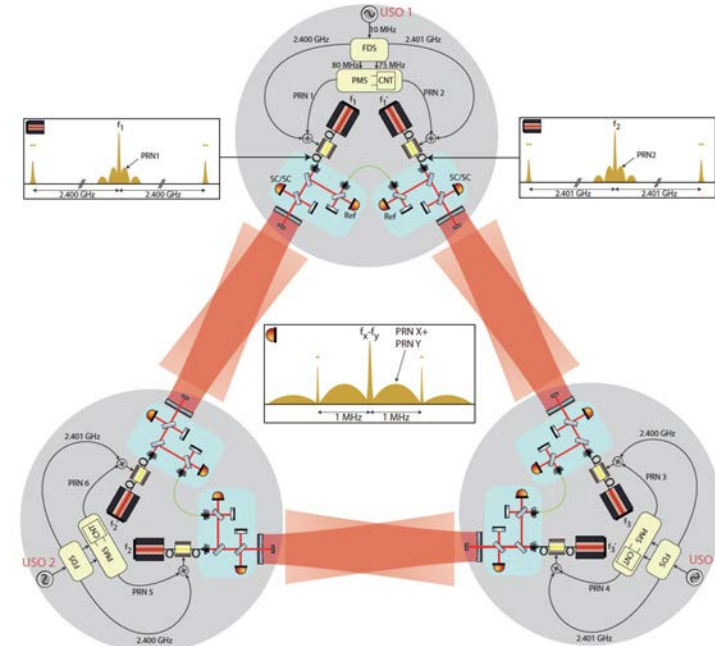
- Residual noise due

$$\frac{\Delta v}{v_0}$$

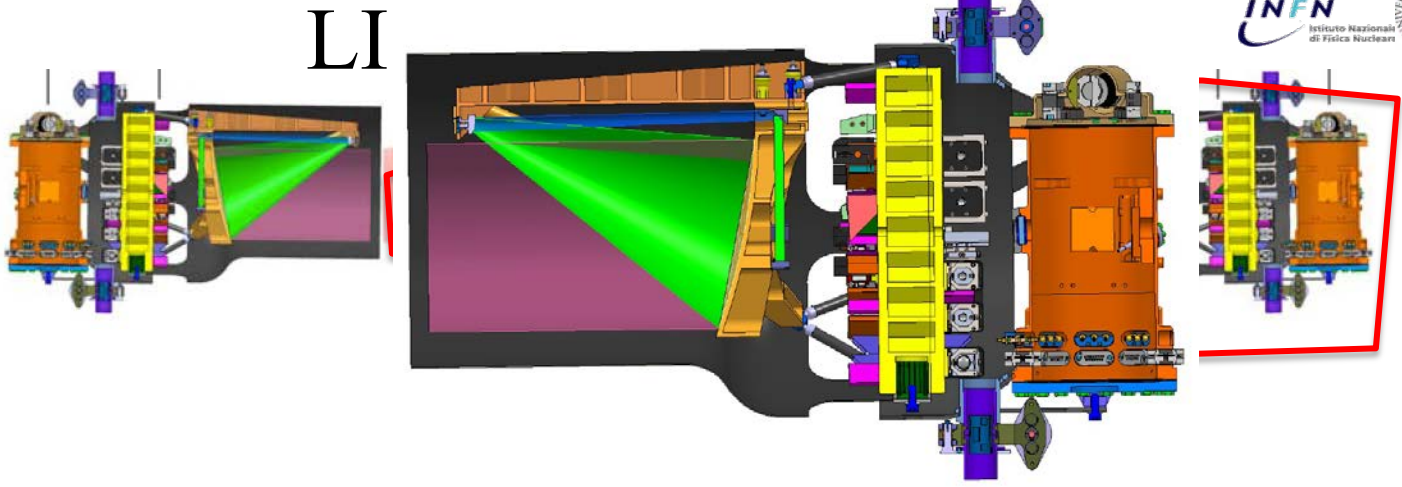
# LISA interferometry



- The LISA arm: two counter-propagating links.
- LISA 3 arms: 6 single-link frequency signals, 100 pW interferometry,  $\approx 10 \text{ pm}/\sqrt{\text{Hz}}$  equivalent test-mass displacement.
- To beat laser noise, data processing requires knowledge of light travel time within 3 ns/1 m. Done with internal “laser GPS”

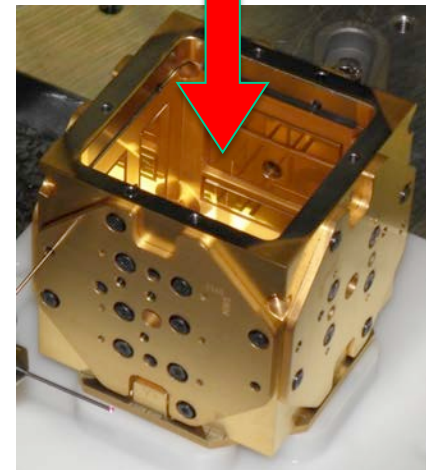
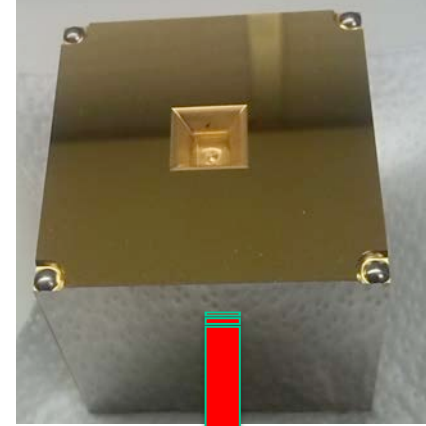
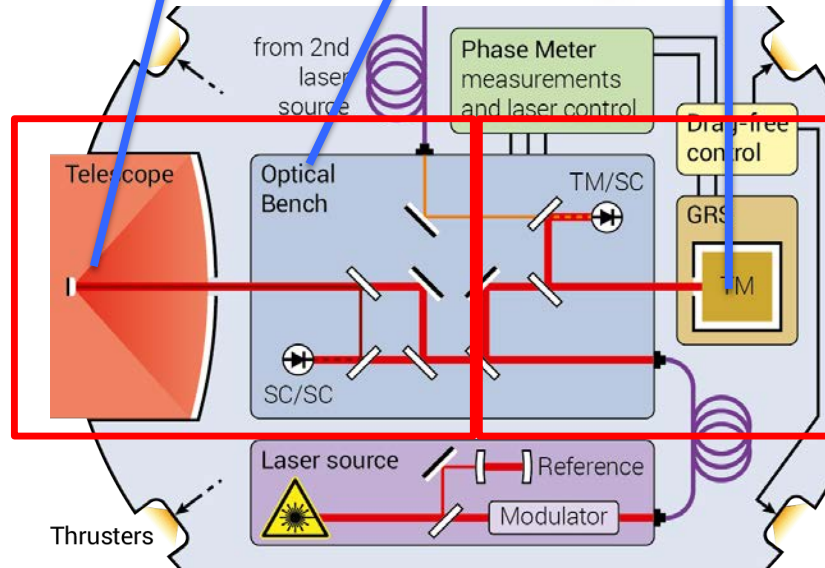
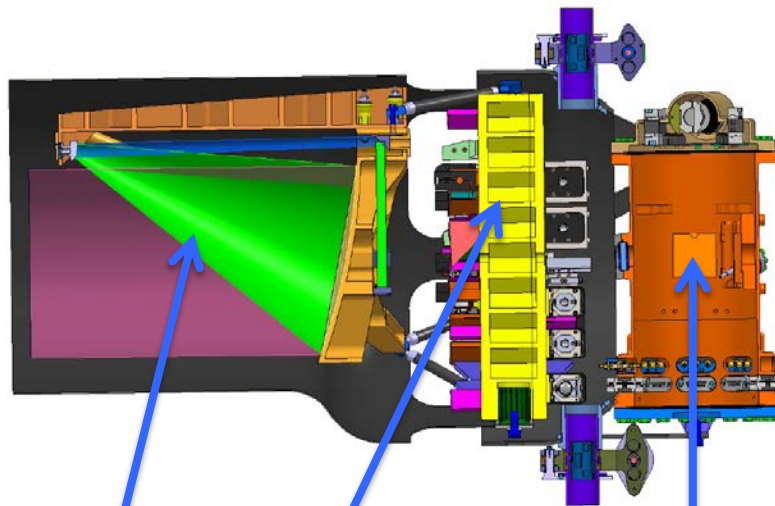




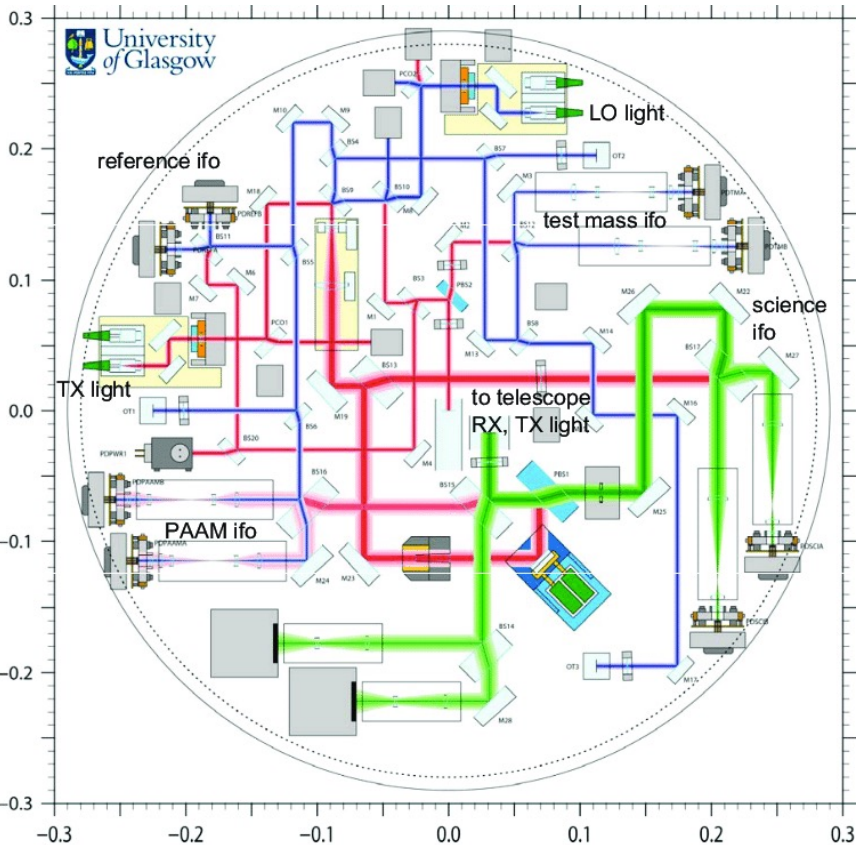


## Instrument

- The Gravitational Reference Sensor with the test-mass
- The Optical Bench with:
  - Local interferometer
  - Spacecraft to spacecraft interferometer, including telescope



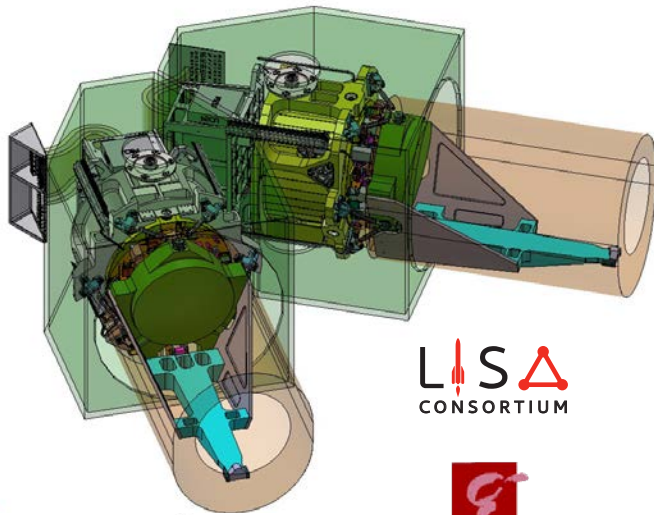
# The optical bench



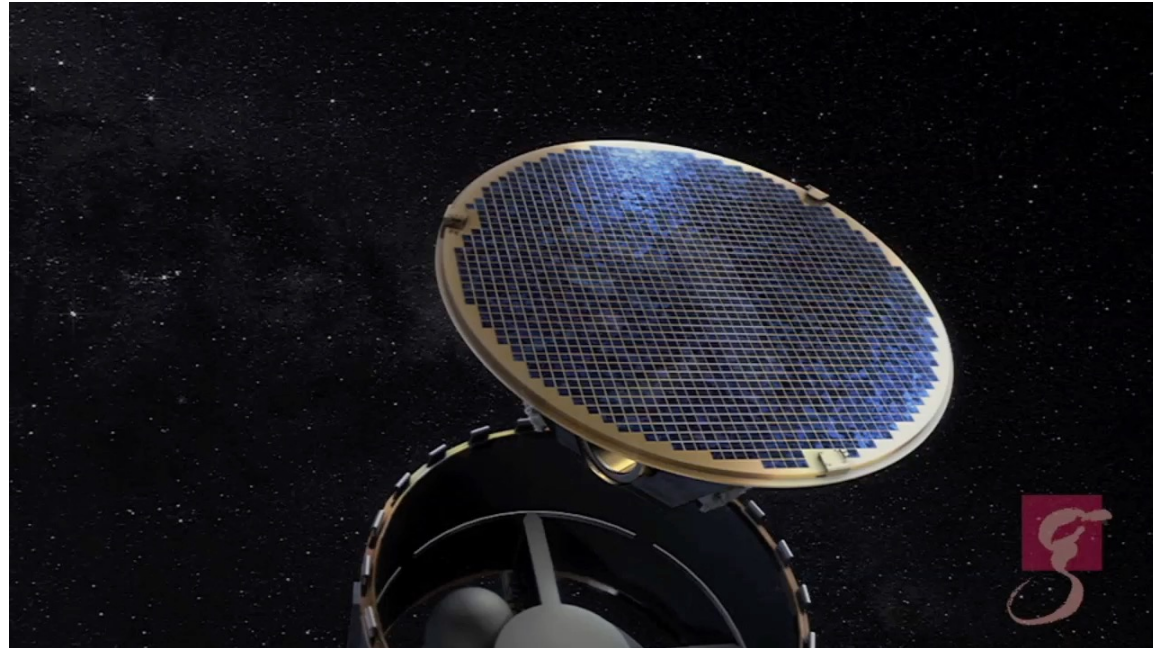
21



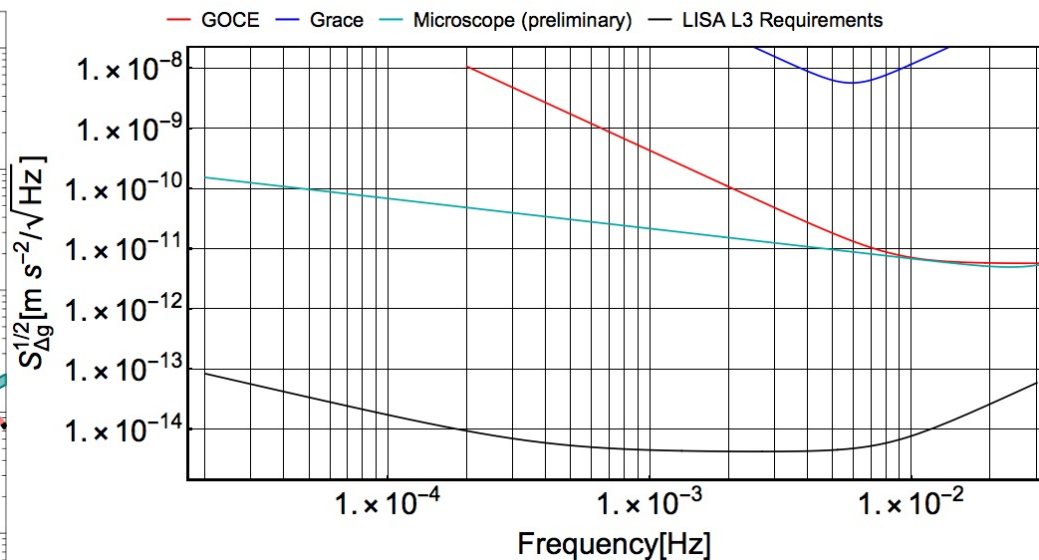
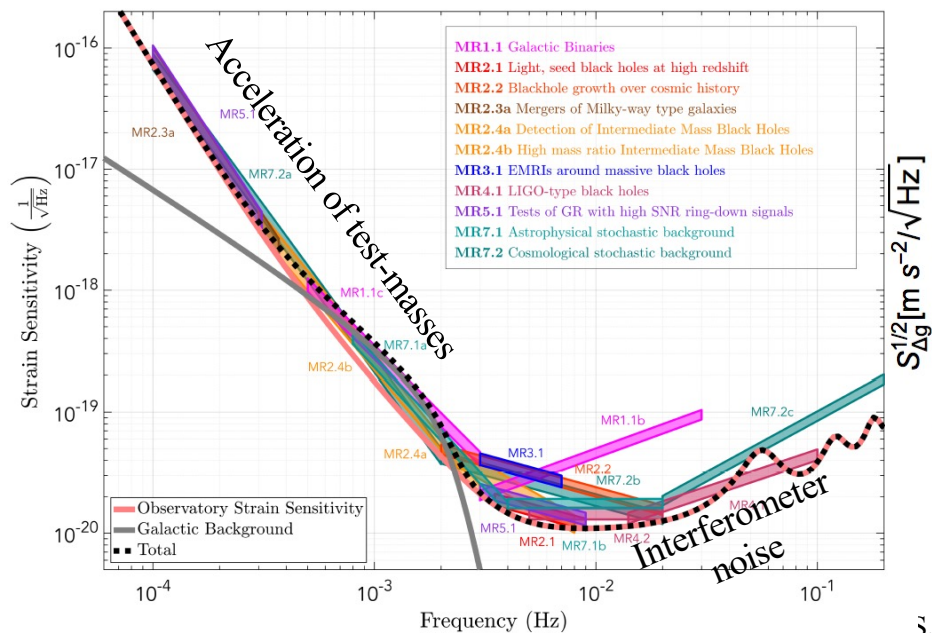
# The full complement



LISA  
CONSORTIUM



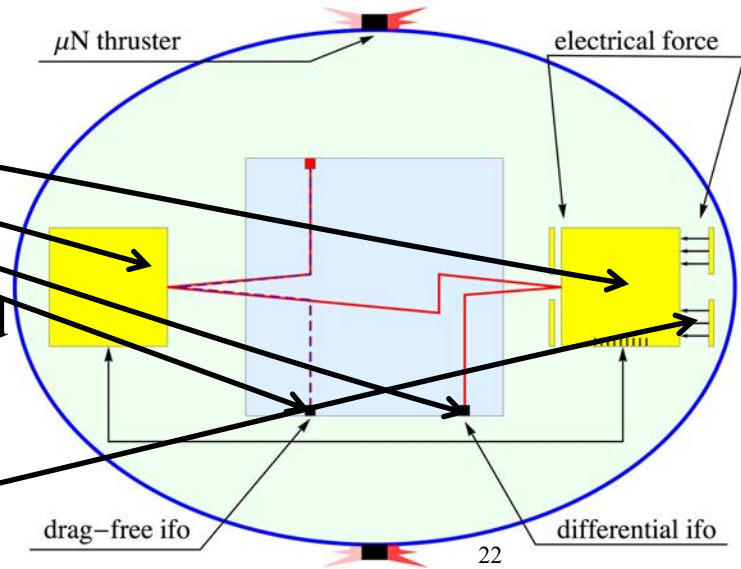
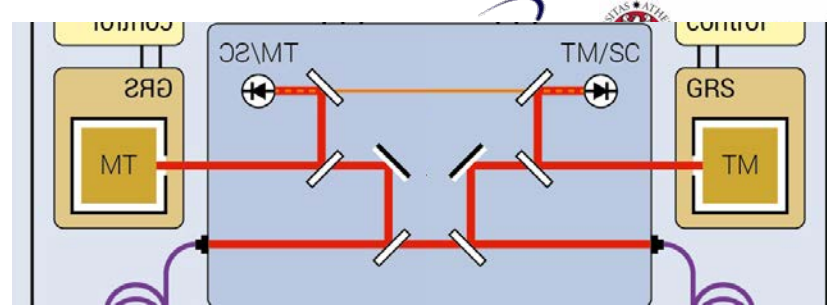
- LISA sensitivity limited at low frequency by acceleration of test-masses
- LISA is a low frequency instrument: much of SNR for most interesting sources accumulated  $\lesssim 10$  mHz
- Acceleration noise  $\leq \text{femto } g/\sqrt{\text{Hz}}$
- Cannot be demonstrated on ground or in LEO





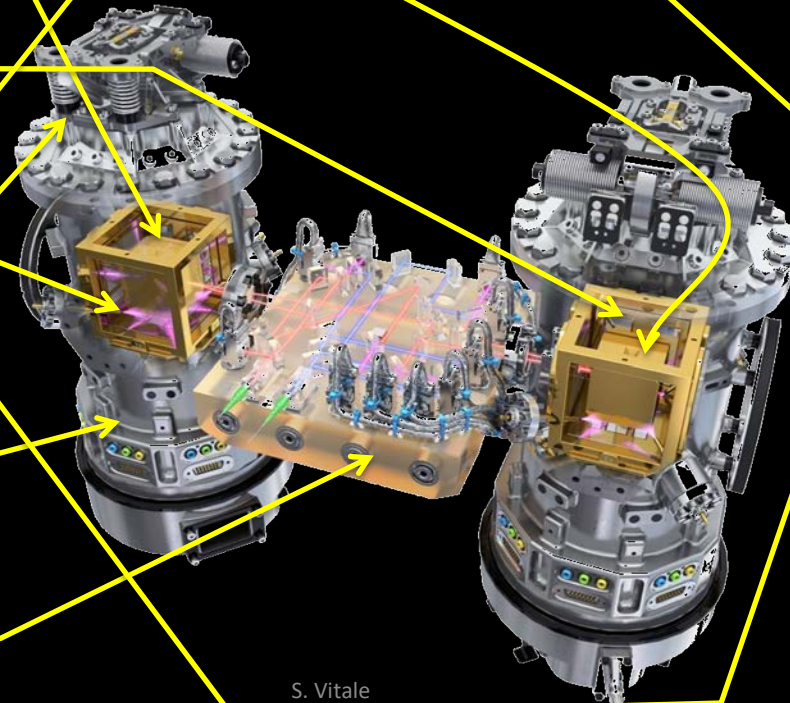
# LISA Pathfinder

- Force disturbance is local. Test does not require million km size
- One LISA link inside a single spacecraft (no million km arm)
- 2 TMs,
- 2 Interferometers (Ifo)
- Satellite chases one test-mass
- Contrary to LISA, second test-mass forced to follow the first at very low frequency by electrostatics

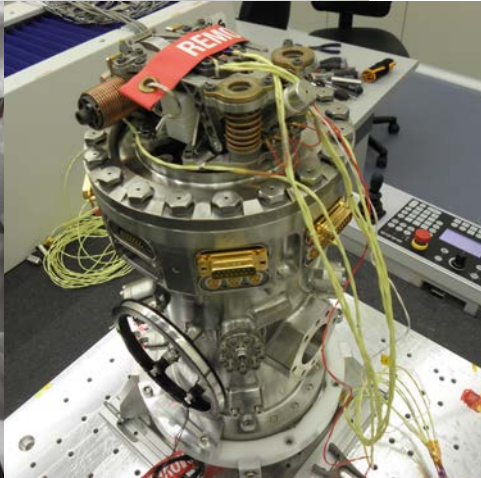
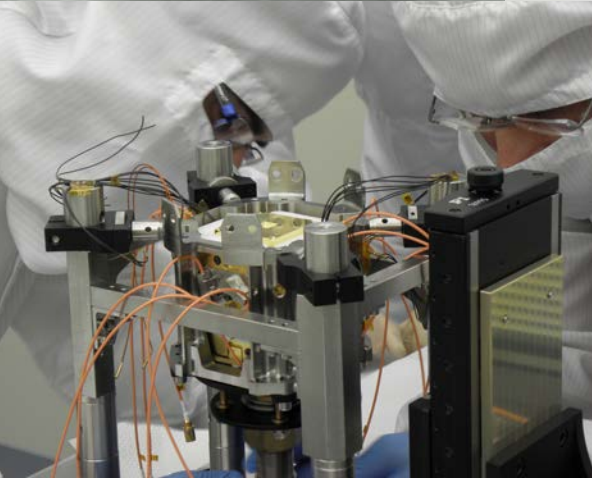
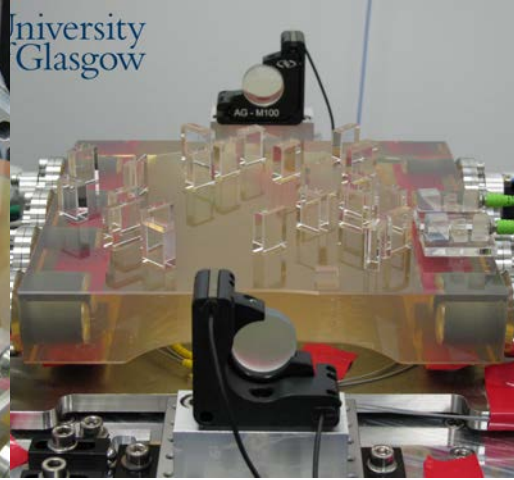
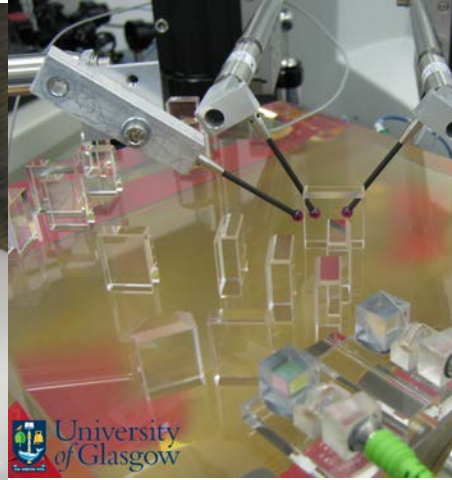
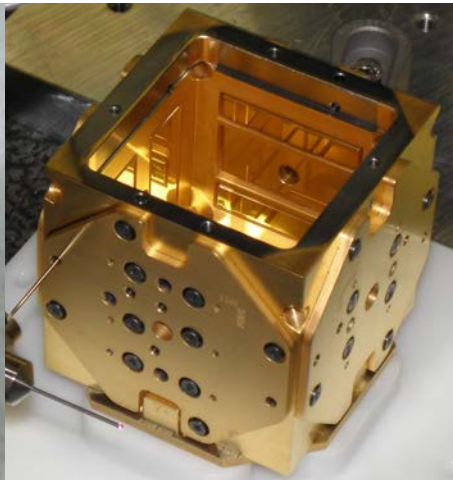
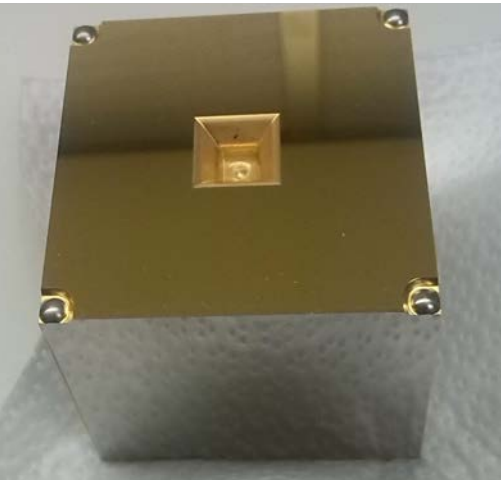


# The LTP

- Test masses gold-platinum, highly non-magnetic, very dense
- Electrode housing: electrodes are used to exert very weak electrostatic force
- UV light, neutralize the charging due to cosmic rays
- Caging mechanism: holds the test-masses and avoid them damaging the satellite at launch
- Vacuum enclosure to handle vacuum on ground
- Ultra high mechanical stability optical bench for the laser interferometer



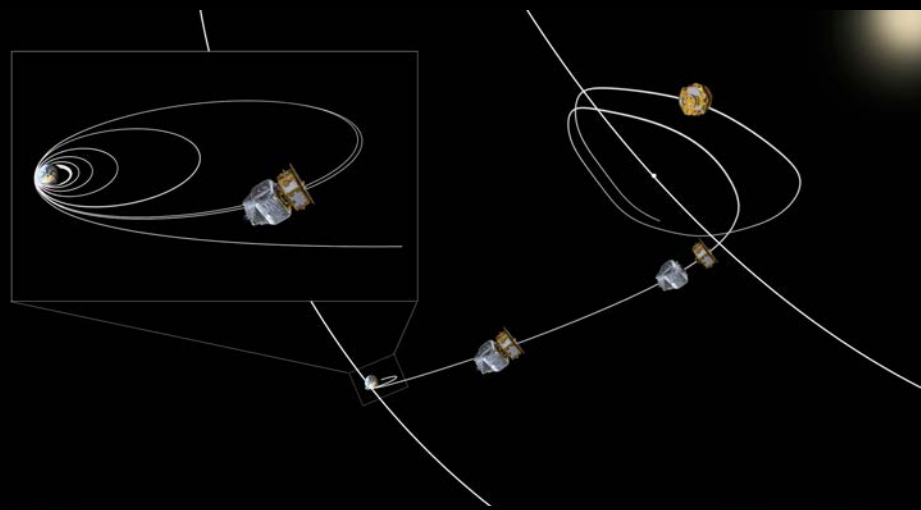
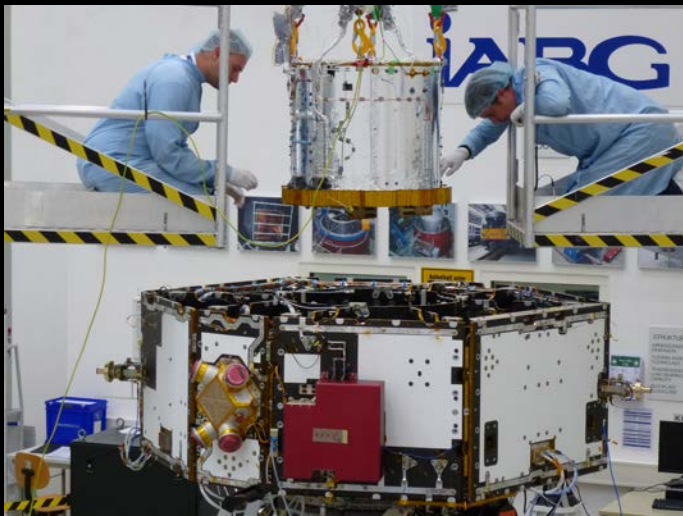
# The real H/W





# Instrument integration



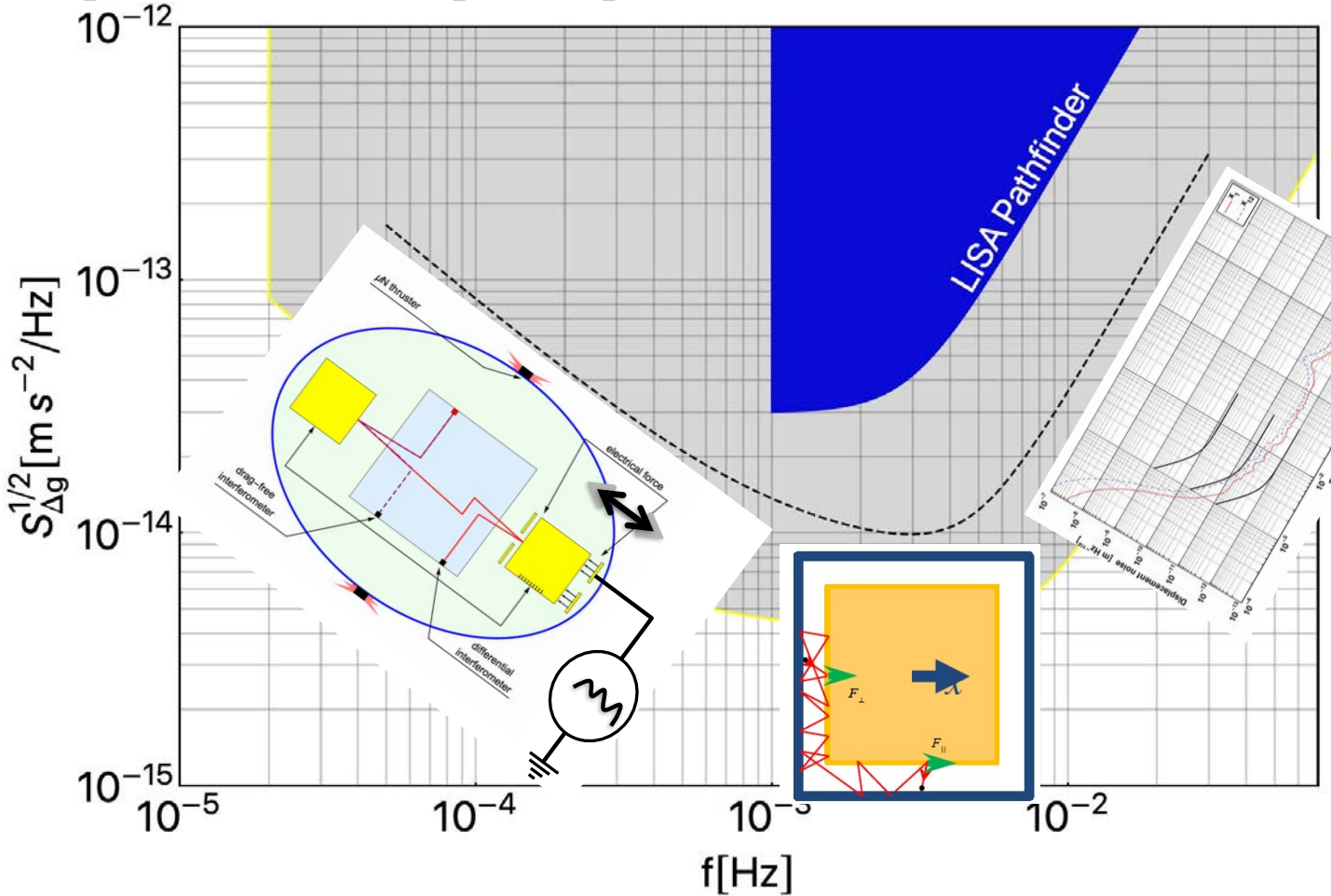


From instrument integration to orbit

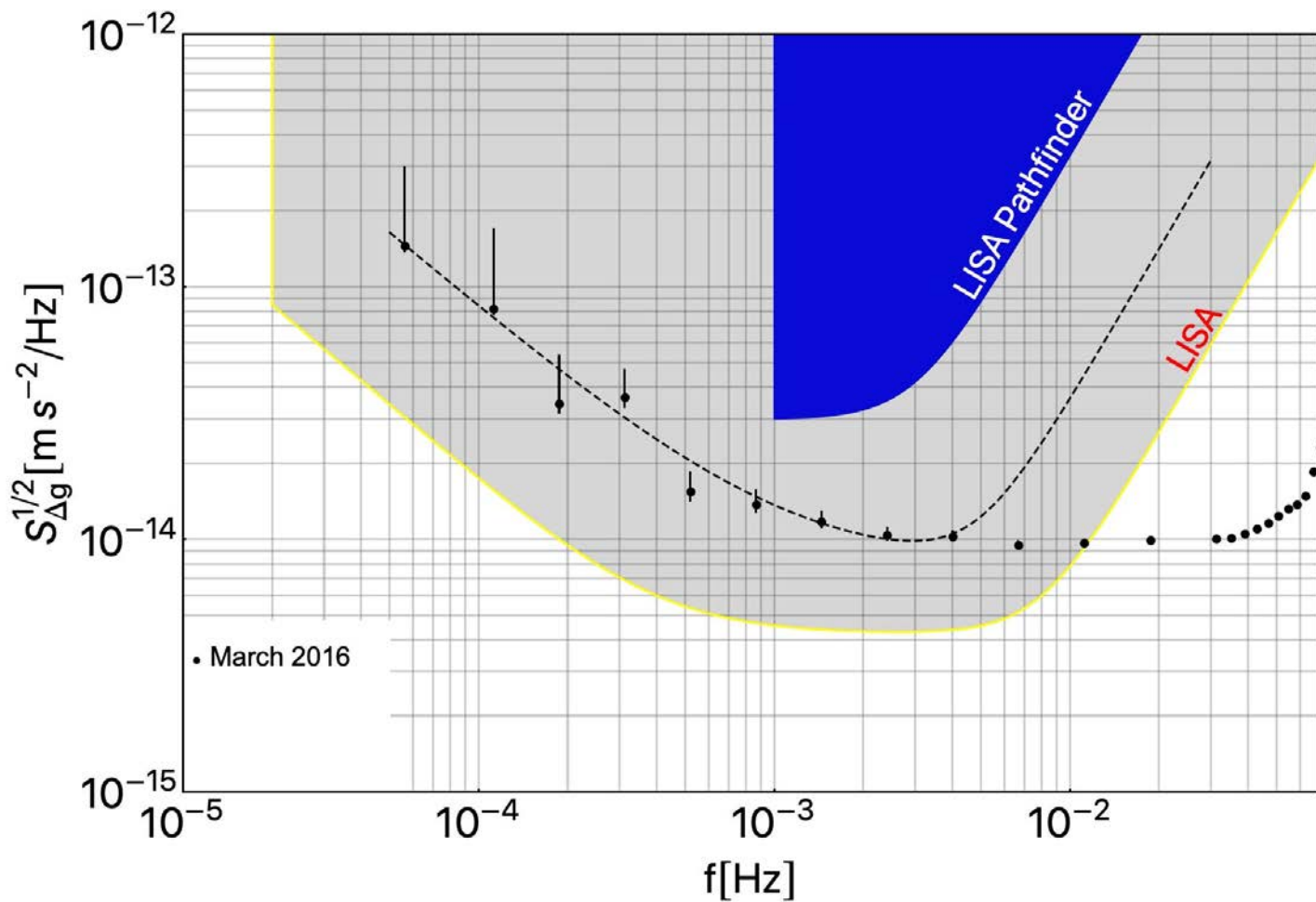


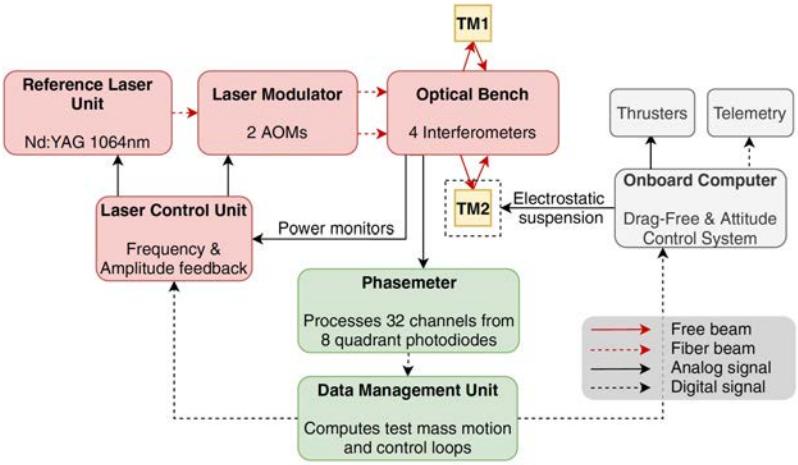
# Requirements and expected performance

- Electrostatic actuation noise:
  - For a given voltage source noise, the larger the needed force you set, the larger the force noise.
  - Required force set by accuracy of gravitational balance
- Brownian noise from residual gas:
  - The larger the pressure surrounding the test-mass the larger the noise
- Interferometer readout noise:  $\approx 10 \text{ pm}/\sqrt{\text{Hz}}$  as for LISA



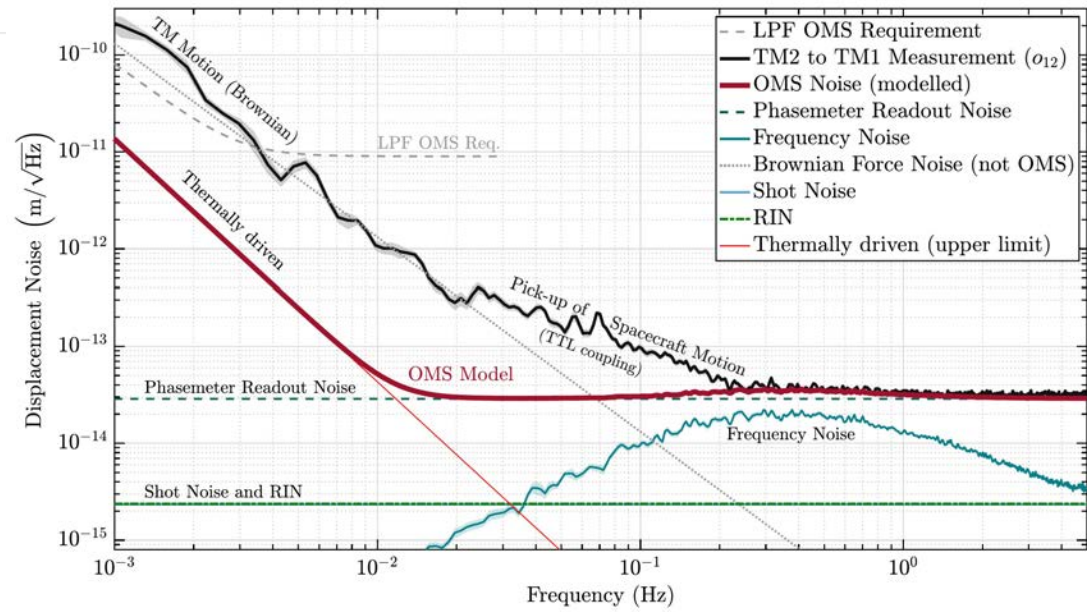
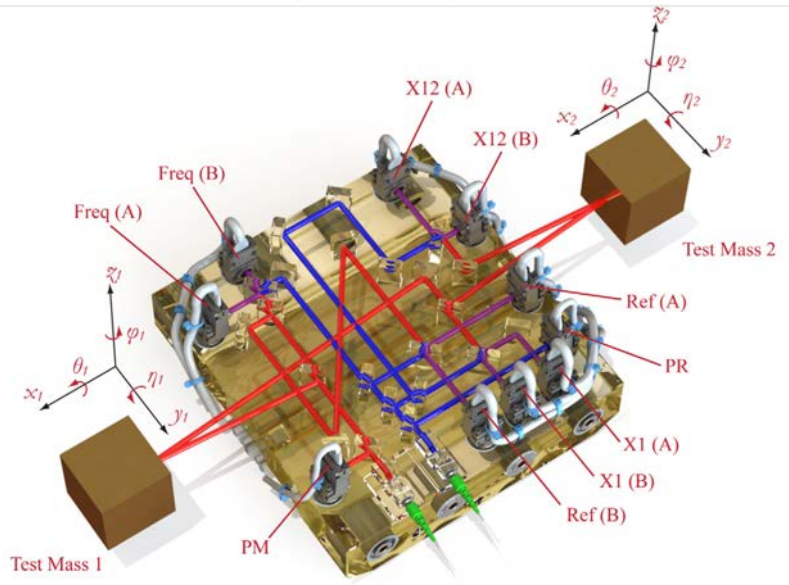
- Close to prediction
- Except for interferometer noise at 35 fm/ $\sqrt{\text{Hz}}$  instead of 10 pm/ $\sqrt{\text{Hz}}$  we could show on ground!





# The magic interferometer

PHYSICAL REVIEW LETTERS 126, 131103 (2021)



# Gravitational control and actuation

- Electrostatic force mostly compensates gravitational force
- Gravitational force canceled in dead reckoning with  $\sim 1.8$  kg balance mass
- Specification  $g_{\max} < 650 \text{ pm s}^{-2}$  ( $3 \sigma + \text{margin}$ )

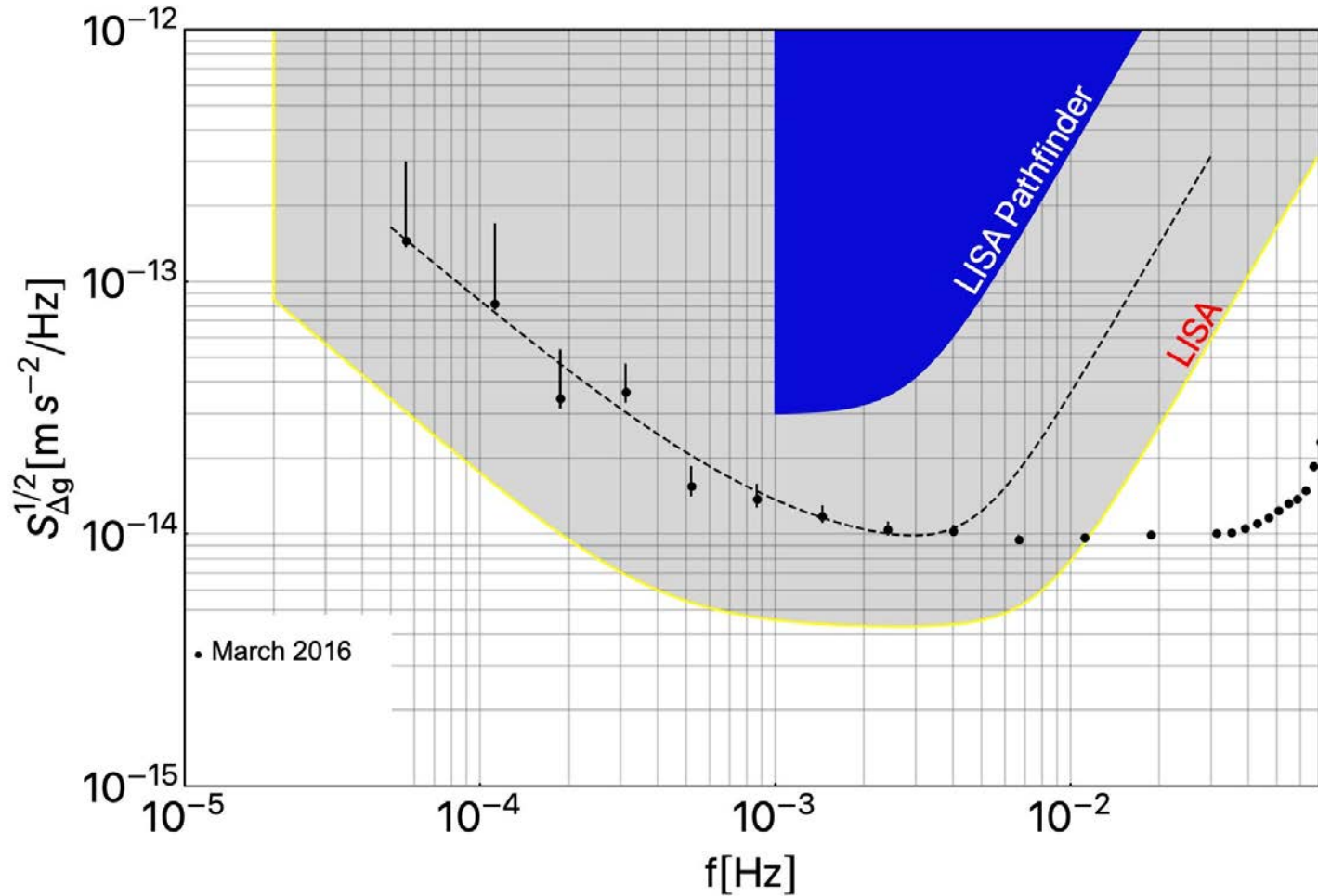
EADS ESA LIBA Pathfinder AVX Mass Tracking Log Page No. 3/4

Line Item	Date	Type	ATS Reference	Description of Name Adjustment (see column 10)	Description of Location	Item Mass [kg]	Item CG [mm]	Temporarily	In Model
1001	2011-01-10	ADD	AVX-001	AVX-001	AVX-001	0.001	0.000		

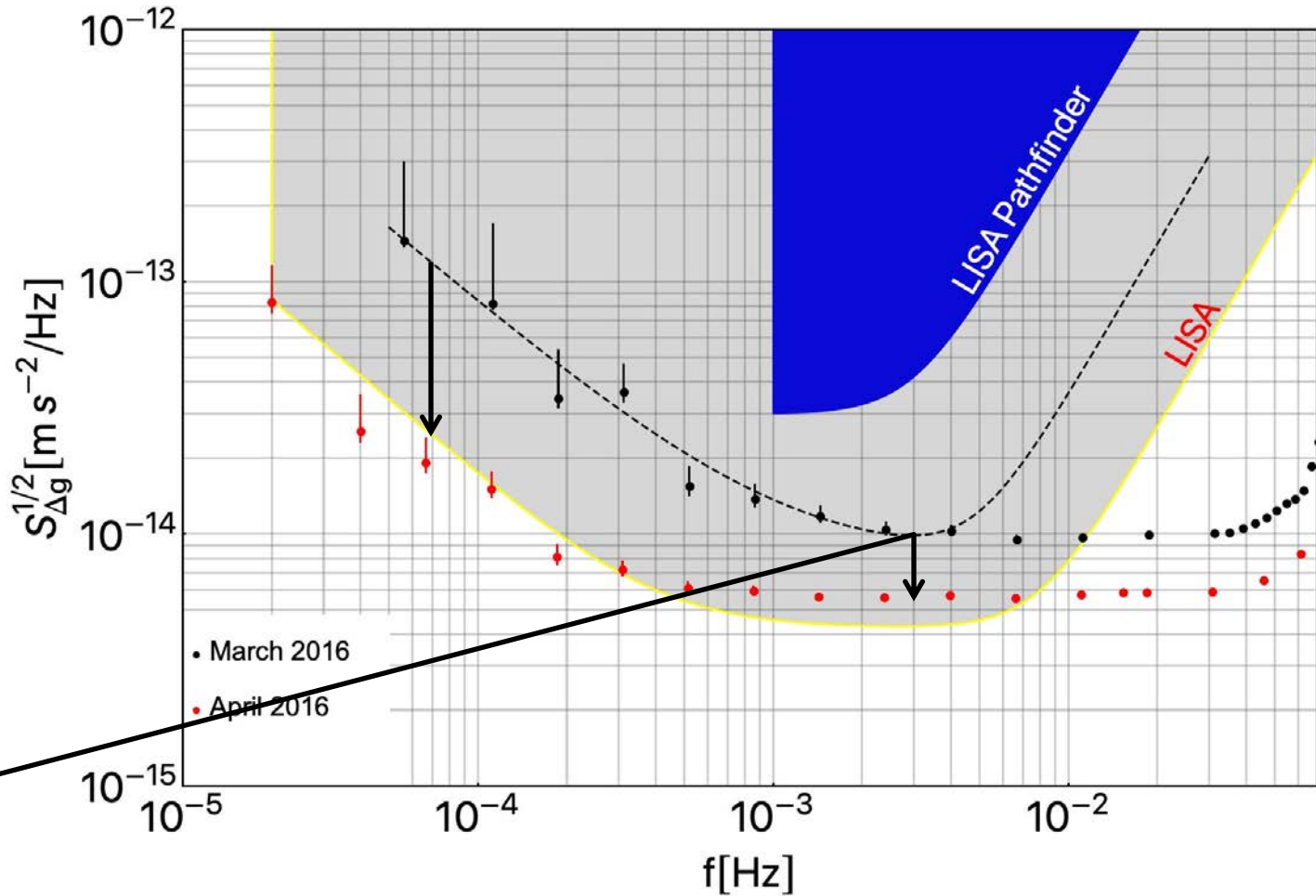
LEVEL	NAME	REMARKS	Min X [m]	Max X [m]	Min Y [m]	Max Y [m]	Min Z [m]	Max Z [m]	Min m [kg]	Max m [kg]	X cog [mm]	Y cog [mm]	Z [mm]
	<b>New Electrode Housing</b>												
	M3 HEXALOBULAR SOCKET SCREW M3x6.4 (D)	Guard ring z- screws (all)	-0.026201	0.026185	-0.026197	0.026182	-0.037475	-0.029135	1.22E-10	2.42E-08	-0.000151604	-0.0003	3
	M3 HEXALOBULAR SOCKET SCREW M3x6.4 (D)	Guard ring z- screws (all)	-0.026201	0.026185	-0.026182	0.026197	-0.029135	0.037475	1.22E-10	2.42E-08	-0.000151604	0.00033	3
	M3 HEXALOBULAR SOCKET SCREW M3x6.4 (D)	Z- cover screws (all)	-0.022529	0.022523	-0.020769	0.020756	-0.043075	-0.034735	1.23E-10	2.35E-08	-7.04325E-05	-0.0003	3
	M3 HEXALOBULAR SOCKET SCREW M3x6.4 (D)	Z+ cover screws (all)	-0.022529	0.022523	-0.020756	0.020769	0.034735	0.043075	1.23E-10	2.35E-08	-7.04325E-05	0.00027	3
	M3 HEXALOBULAR SOCKET SCREW 3X6.4 (A)	X- face screws	0.029662	0.037972	-0.030199	0.030198	-0.029194	0.029191	9.41E-11	3.64E-08	34.36440315	-0.0001	6
	M3 HEXALOBULAR SOCKET SCREW 3X6.4 (A)	X+ face screws	-0.037972	-0.029662	0.030198	0.030199	-0.029194	0.029191	9.41E-11	3.64E-08	-34.36440315	0.0001	6
	M3 HEXALOBULAR SOCKET SCREW 3X6.4 (A)	Y- face screws	-0.032203	0.032203	0.028562	0.036872	-0.030198	0.030197	9.41E-11	3.64E-08	-9.38224E-05	33.2644	0
	M3 HEXALOBULAR SOCKET SCREW 3X6.4 (A)	Y+ face screws	-0.032203	0.032203	-0.036872	-0.028562	-0.030198	0.030197	9.41E-11	3.64E-08	9.38224E-05	-33.2644	0
	M3 HEXALOBULAR SOCKET SCREW 3X6.4 (A)	Z- face screws	-0.032993	0.032993	-0.032991	0.032991	-0.037472	-0.029162	9.41E-11	3.64E-08	-0.000201659	-1.1E-05	3
	M3 HEXALOBULAR SOCKET SCREW 3X6.4 (A)	Z+ face screws	-0.032993	0.032993	-0.032991	0.032991	0.029162	0.037472	9.41E-11	3.64E-08	-0.000201659	1.1E-05	3
	M3 HEXALOBULAR SOCKET SCREW 3X6.9 (B)	y+ dir	0.034734	0.043568	-0.019636	-0.015239	-0.006856	-0.002459	1.18E-10	2.39E-08	39.75527429	-17.436	-4
	M3 HEXALOBULAR SOCKET SCREW 3X6.9 (B)		0.034734	0.043568	0.015239	0.019636	-0.006856	-0.002459	1.18E-10	2.39E-08	39.75527429	17.4358	-4
	M3 HEXALOBULAR SOCKET SCREW 3X6.9 (B)		-0.043568	-0.034734	0.015239	0.019636	-0.006856	-0.002459	1.18E-10	2.39E-08	-39.75527429	17.4358	-4
	M3 HEXALOBULAR SOCKET SCREW 3X6.9 (B)		-0.043568	-0.034734	-0.019636	-0.015239	-0.006856	-0.002459	1.18E-10	2.39E-08	-39.75527429	-17.436	-4
	M3 HEXALOBULAR SOCKET SCREW 3X6.9 (B)	all y- cover screws	-0.011346	0.001784	0.033634	0.042468	-0.010393	0.010171	1.18E-10	2.45E-08	-3.854340843	38.6552	-
	M3 HEXALOBULAR SOCKET SCREW 3X6.9 (B)	all y+ cover screws	-0.001784	0.011346	-0.042468	-0.033634	-0.010393	0.010171	1.18E-10	2.45E-08	3.854340843	-38.6552	-
	EH Frame		-0.035911	0.03592	-0.035923	0.03592	-0.034455	0.034464	1.58E-10	5.32E-07	0.168660707	-0.0001	0
	Z+ Face Assy												



# Authority 65 pico g

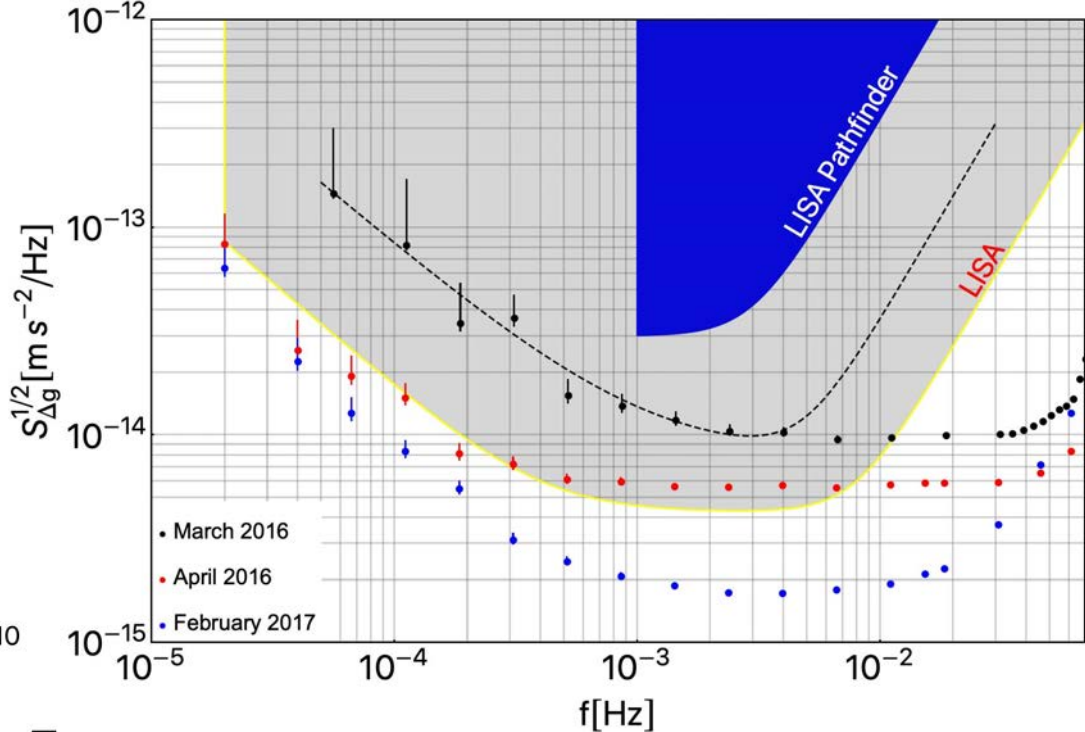
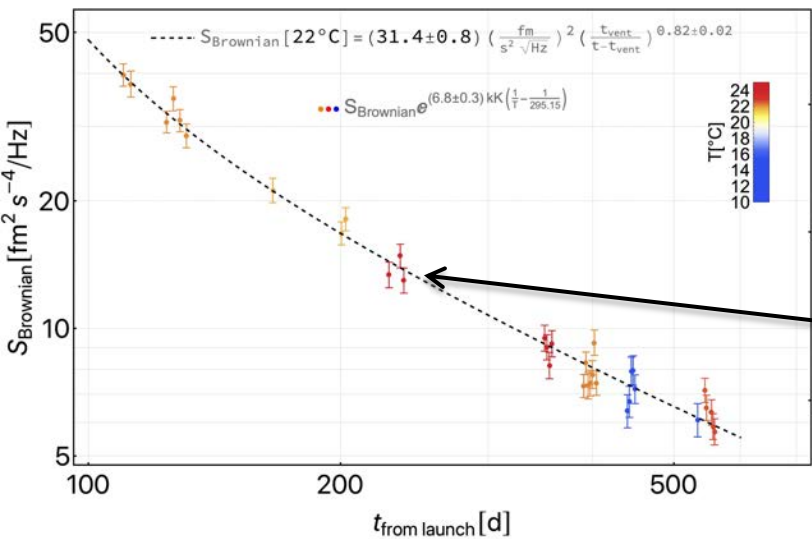


- Brownian noise decreases with pressure as the system is vented to outer space





# LISA requirements met with some margin



Brownian noise (pressure) vs time throughout the mission

# Consolidating the noise model: LPF full menu of experiments

- [1] M. Armano, et al. Sub-femto- $g$  free fall for space-based gravitational wave observatories: Lisa pathfinder results. *Phys. Rev. Lett.*, 116:231101, Jun 2016.
- [2] D. Vetrugno et al. Lisa pathfinder first results. *International Journal of Modern Physics D*, 26(05):1741023, 2017.
- [3] M. Armano, et al. Charge-induced force noise on free-falling test masses: Results from lisa pathfinder. *Phys. Rev. Lett.*, 118:171101, Apr 2017.
- [4] M. Armano, et al. Capacitive sensing of test mass motion with nanometer precision over millimeter-wide sensing gaps for space-borne gravitational reference sensors. *Phys. Rev. D*, 96:062004, Sep 2017.
- [5] M. Armano, et al. Characteristics and energy dependence of recurrent galactic cosmic-ray flux depressions and of a forrush decrease with LISA pathfinder. *The Astrophysical Journal*, 854(2):113, Feb 2018.
- [6] M. Armano, et al. Beyond the required lisa free-fall performance: New lisa pathfinder results down to 20  $\mu\text{Hz}$ . *Phys. Rev. Lett.*, 120:061101, Feb 2018.
- [7] M. Armano, et al. Calibrating the system dynamics of lisa pathfinder. *Phys. Rev. D*, 97:122002, Jun 2018.
- [8] M. Armano, et al. Precision charge control for isolated free-falling test masses: Lisa pathfinder results. *Phys. Rev. D*, 98:062001, Sep 2018.
- [9] G. Anderson, et al. Experimental results from the st7 mission on lisa pathfinder. *Phys. Rev. D*, 98:102005, Nov 2018.
- [10] M. Armano, et al. Forrush decreases and  $<2$  day GCR flux non-recurrent variations studied with LISA pathfinder. *The Astrophysical Journal*, 874(2):167, apr 2019.
- [11] M. Armano, et al. Lisa pathfinder platform stability and drag-free performance. *Phys. Rev. D*, 99:082001, Apr 2019.
- [12] M Armano, et al. Temperature stability in the sub-milliHertz band with LISA Pathfinder. *Monthly Notices of the Royal Astronomical Society*, 486(3):3368–3379, 04 2019.
- [13] M. Armano, et al. Lisa pathfinder microneutron cold gas thrusters: In-flight characterization. *Phys. Rev. D*, 99:122003, Jun 2019.
- [14] M. Armano, et al. Lisa pathfinder performance confirmed in an open-loop configuration: Results from the free-fall actuation mode. *Phys. Rev. Lett.*, 123:111101, Sep 2019.
- [15] J. I. Thorpe, et al. Micrometeoroid events in LISA pathfinder. *The Astrophysical Journal*, 883(1):53, sep 2019.
- [16] M. Armano, et al. Novel methods to measure the gravitational constant in space. *Phys. Rev. D*, 100:062003, Sep 2019.
- [17] M. Armano, et al. Analysis of the accuracy of actuation electronics in the laser interferometer space antenna pathfinder. *Review of Scientific Instruments*, 91(4):045003, 2020.
- [18] M Armano, et al. Spacecraft and interplanetary contributions to the magnetic environment on-board LISA Pathfinder. *Monthly Notices of the Royal Astronomical Society*, 494(2):3014–3027, 04 2020.
- [19] M. Armano, et al. Sensor noise in lisa pathfinder: In-flight performance of the optical test mass readout. *Phys. Rev. Lett.*, 126:131103, Apr 2021.

# Phase A Conclusions – MFR outcome

## Timeline



October 2013:  
 October 2016:  
**June 2017:**  
 May 2018:  
**2018-2021:**  
**Oct '20-Oct '21:**

April 2022	Phase B1 Kick-Off (New Requirements Architecture ready)
6. C Q4 / 2022	Intermediate Review (Consolidation of requirements to CFIs)
<del>Q4 / 2023</del>	<del>Mission Adoption Review</del>
<del>Q1 / 2024</del>	<del>Mission Adoption (TBC)</del>

**Q2 / 2023 Instrument SRR ("Adoption review for CFIs")**

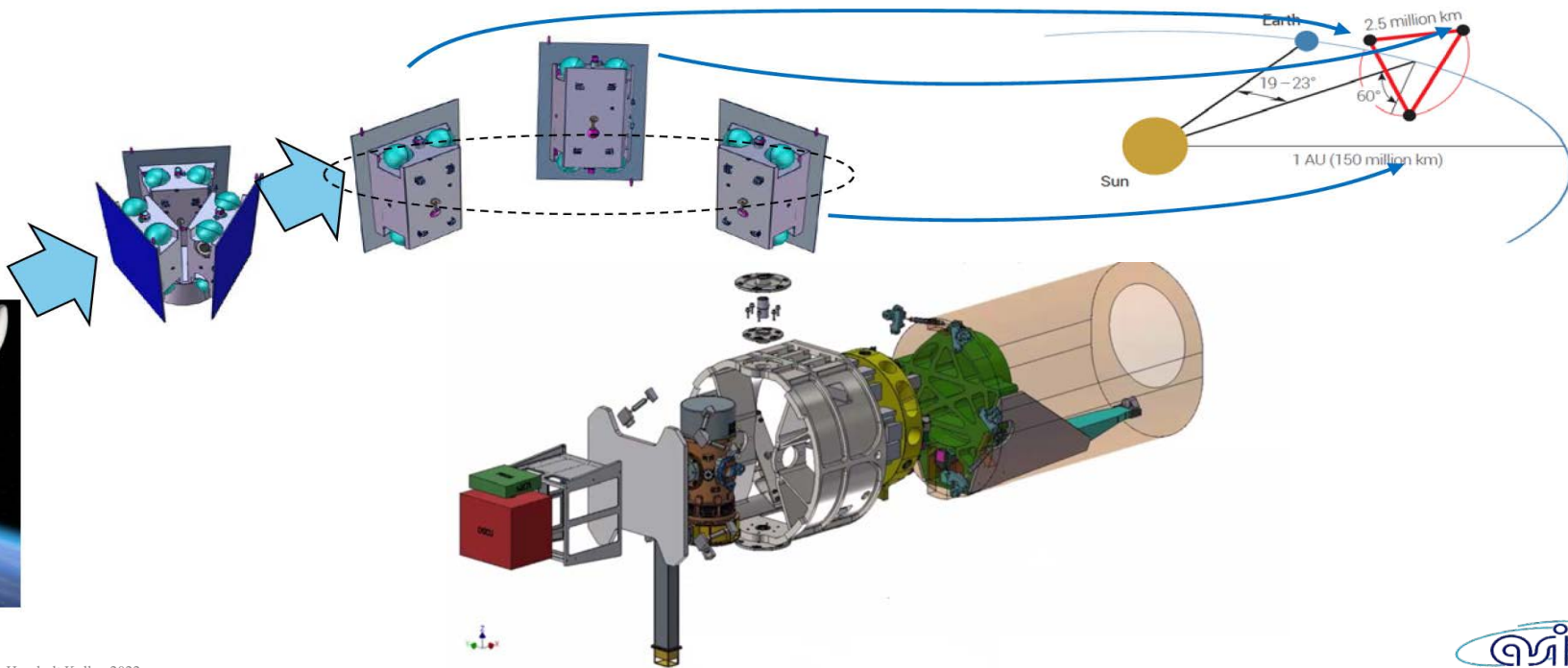
**Q3 2023**

**Q4 2023**

<end 2021: Formulation Review (end Phase A)  
 >2021: Mission Phase B1  
 <2024: Mission Adoption  
 >Adoption: Mission Implementation (Phase B2/C/D)  
 <2034: Launch  
 >Launch: 6.5 years operations (+6 years potential extension)

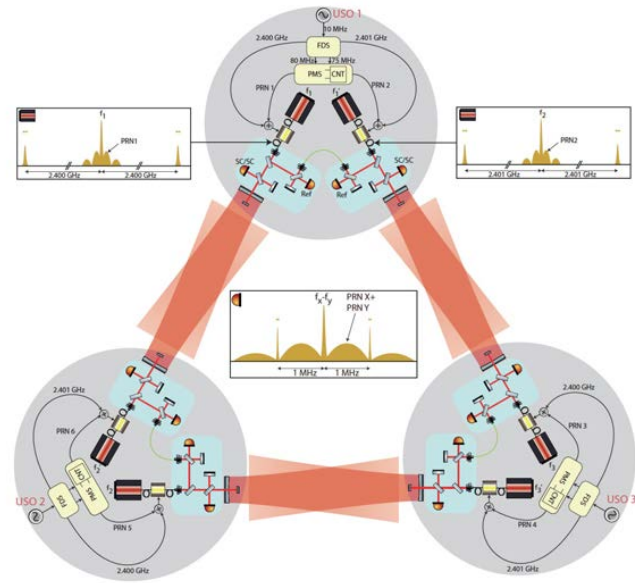
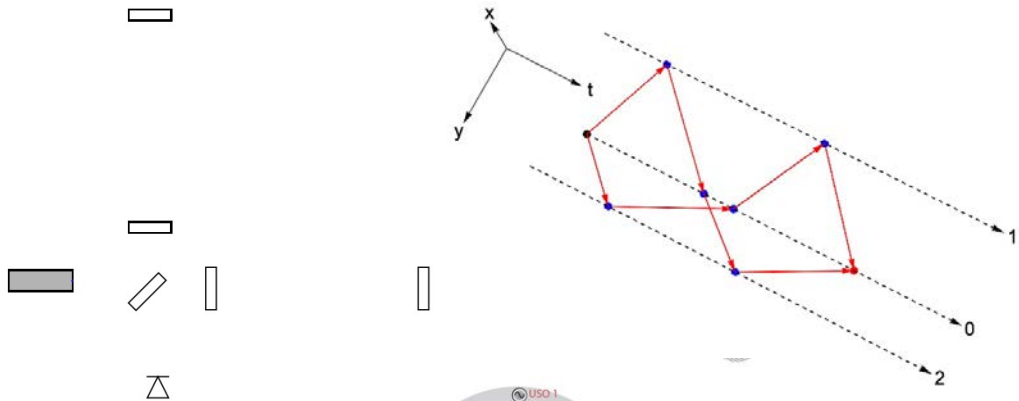
# LISA currently in phase B1

- Phase-A study competitive: cannot show much!
- A rather stable concept, working out the details



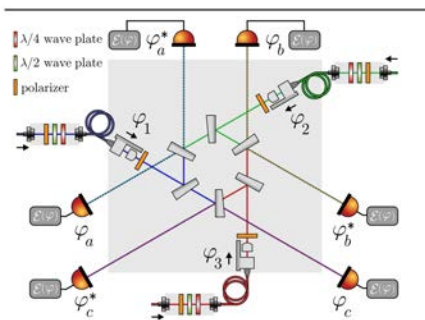
# Laser frequency noise & time delay interferometry

- Laser frequency stability:
  - Required  $\approx 1 \mu\text{Hz}/\sqrt{\text{Hz}}$
  - Available  $\leq 30 \text{ Hz}/\sqrt{\text{Hz}}$
- Ground based interferometers beat noise comparing beams emitted at same time (equal arms)
- LISA: arms are unequal ( $\Delta L \approx 10^5 \text{ km}$ ) and time varying over the year.
- Combine single-link signals to mimic light beams that have traveled equal lengths

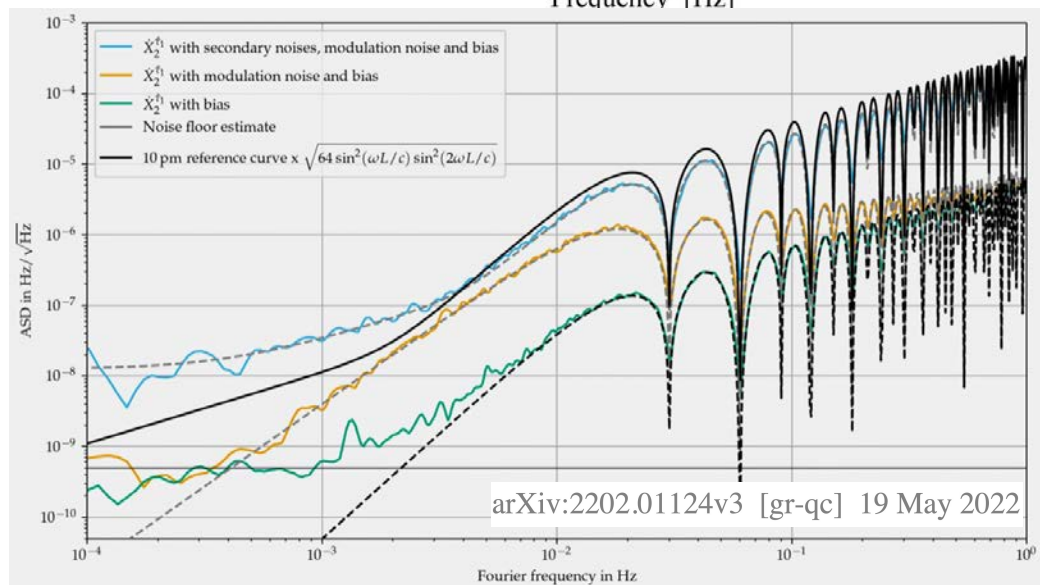
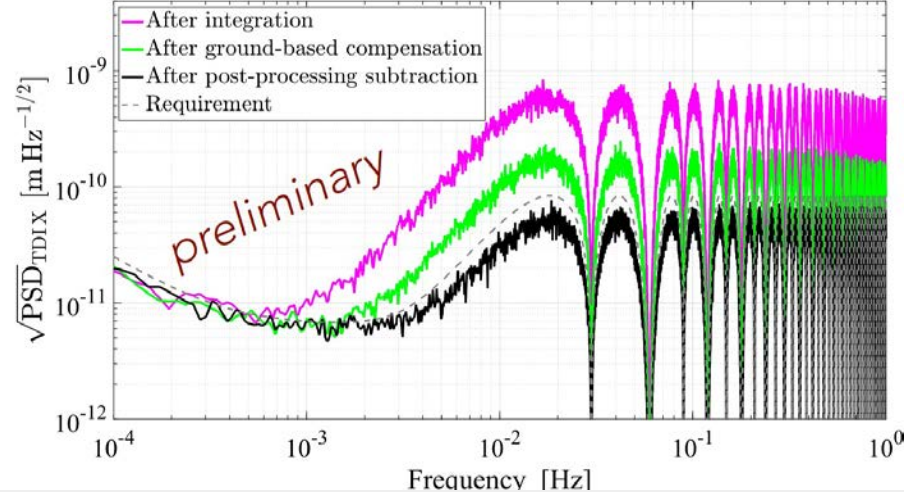
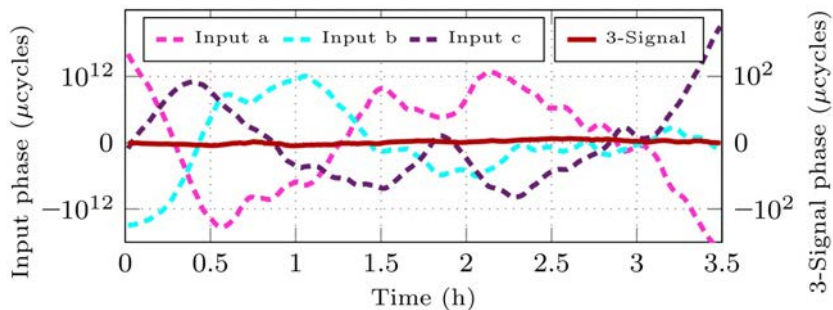


# Progress on Interferometry

- Beating misalignments
- Beating frequency and clock noise

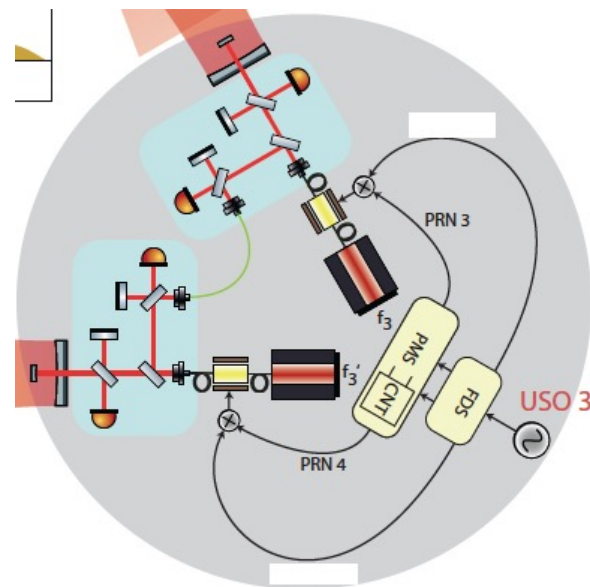
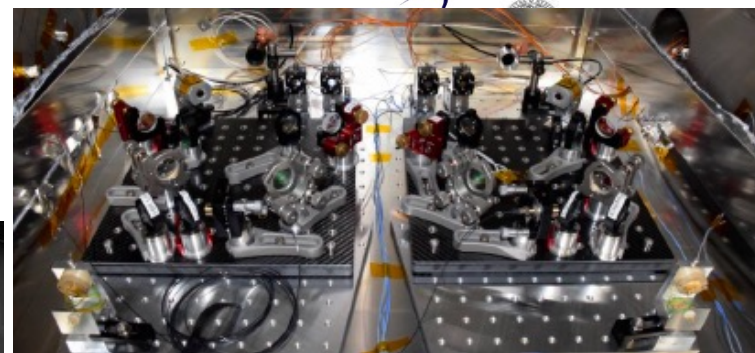
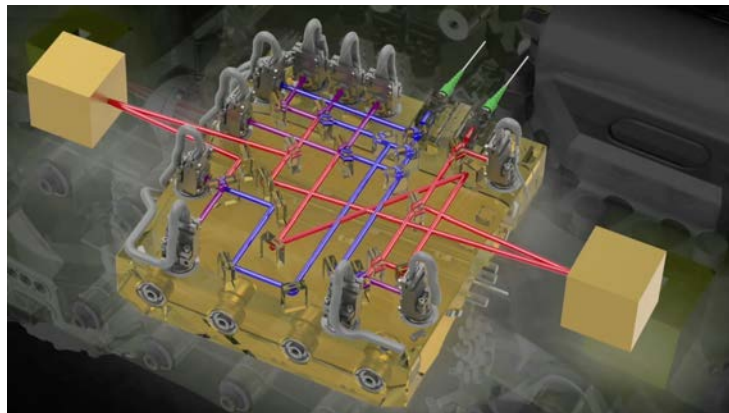
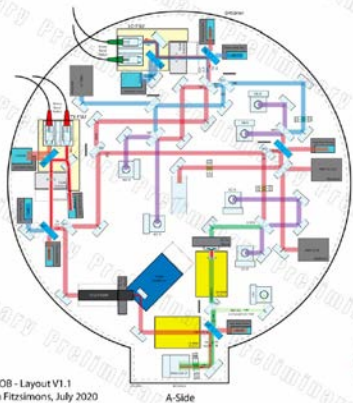


PHYSICAL REVIEW LETTERS **122**, 081104 (2019)

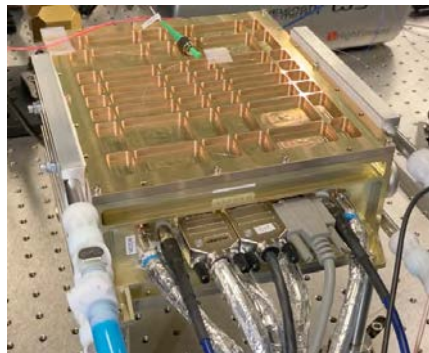


arXiv:2202.01124v3 [gr-qc] 19 May 2022

# Technology developments (TRL 6 by adoption)



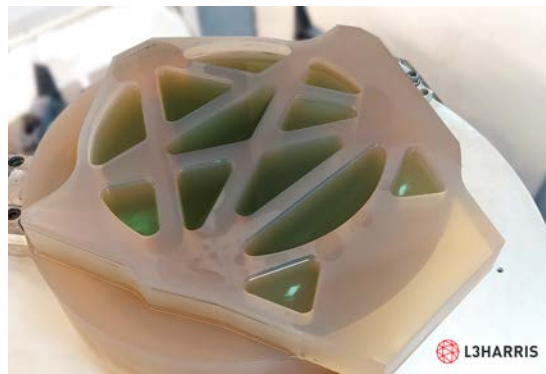
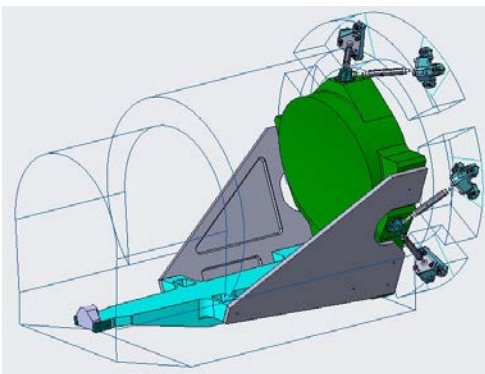
# Technology developments (TRL6 by adoption)



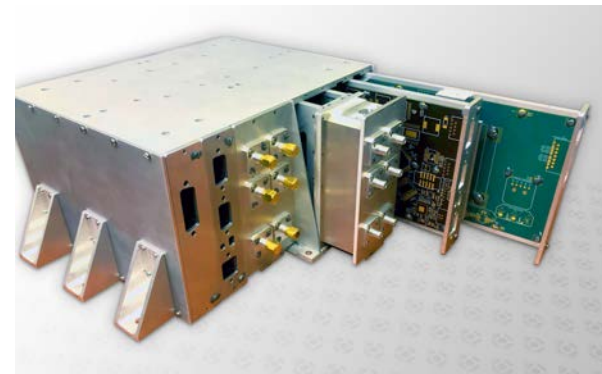
Laser



Telescope



Charge management









Thank you!

MUSE